

# Cautious Optimizers: Improving Training with One Line of Code

Kaizhao Liang<sup>1</sup> Lizhang Chen<sup>1</sup> Bo Liu<sup>1</sup> Qiang Liu<sup>1</sup>

## Abstract

AdamW has been the default optimizer for transformer pretraining. For many years, our community searches for faster and more stable optimizers with only constraint positive outcomes. In this work, we propose a **single-line modification in Pytorch** to any momentum-based optimizer, which we rename Cautious Optimizer, e.g. C-AdamW and C-Lion. Our theoretical result shows that this modification preserves Adam’s Hamiltonian function and it does not break the convergence guarantee under the Lyapunov analysis. In addition, a whole new family of optimizers is revealed by our theoretical insight. Among them, we pick the simplest one for empirical experiments, showing speed-up on Llama and MAE pretraining up to  $1.47\times$ .<sup>1</sup>

## 1. Introduction

Optimization is an important and constantly evolving field in modern machine learning. Undoubtedly, Adam (Kingma, 2014) and AdamW (Loshchilov, 2017) are the most consequential optimizers proposed almost a decade ago. Since then, many efforts (Zhang et al., 2021; Loshchilov et al., 2017) have been made to discover better and faster optimizers beyond these two. However, until now, AdamW remains the dominant workhorse for applications, from pre-training Large Language Models (LLMs) (Touvron et al., 2023) to fine-tuning text to image diffusion (Rombach et al., 2022), with no real challenges to their ruling status.

In the dawn of the era of LLMs, the arms race of model scaling intensifies (Achiam et al., 2023). A faster optimizer means more training tokens can be consumed within the same amount of time. Ultimately, this leads to more capable models (Kaplan et al., 2020). Hence, the interest in searching for an optimizer beyond AdamW is re-kindled. Recent progress in new AdamW alternatives such as LION (Chen et al., 2024; 2023a), SHAMPOO (Gupta et al., 2018), and SOAP (Vyas et al., 2024), ADOPT (Taniguchi et al., 2024), and Schedule-Free (Defazio et al., 2024), all claim substantial improvement over AdamW.

<sup>1</sup>Code is available at <https://github.com/kyleliang919/C-Optim>

## Algorithm 1 Caution an Optimizer (OPT) in PyTorch

```
# param p, update u from OPT, grad g
m = (u * g > 0).to(g.dtype)
p.add_(u * m / (m.mean() + eps), alpha=-lr)
```

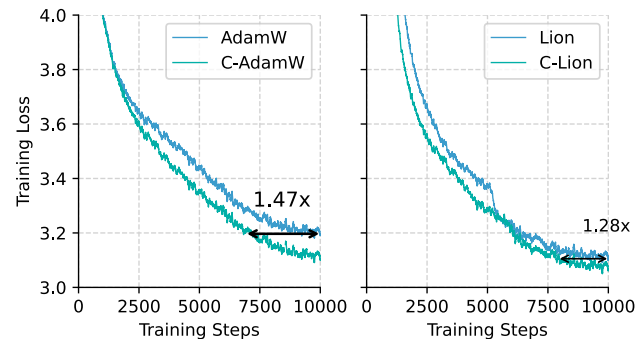


Figure 1: Training Loss Curves on LLaMA 1B, using AdamW / Lion and their cautious variants (using Algorithm 1). The cautious variants achieve better convergence and are  $1.47\times$  and  $1.28\times$  more sample efficient for AdamW and Lion respectively.

However, these methods are either significantly more expensive or require non-trivial efforts to obtain optimal results, especially hyperparameter tuning, which greatly limits their potential and wide adoption. In light of this dilemma, we propose *cautious optimizers*, an exceptionally simple performance booster of any momentum-based optimizer that only requires one line of modification (see Algorithm 1). The change is simple: *do not update unless the proposed update direction and the current gradients are aligned*. With this minor change, we obtain universal improvement over the base optimizer without modification of the original optimal hyperparameters. For example, the cautious versions of AdamW and Lion, denoted as C-AdamW, and C-Lion, respectively, gain  $1.47\times$  and  $1.28\times$  speedups on Llama 1B with virtually no overhead (see Figure 1).

To give an overview of the idea, let us consider a general optimizer for minimizing loss  $\mathcal{L}(w)$ :

$$w_{t+1} \leftarrow w_t - \epsilon_t u_t,$$

where  $u_t$  is the negative update direction of the parameter  $w_t$  at iteration  $t$  and  $\epsilon_t > 0$  the step size. In momentum-based optimizers,  $u_t$  does not necessarily align with the gradient direction  $g_t = \nabla \mathcal{L}(w_t)$ , and hence may cause a

temporary increase of the loss function and slow down the convergence. Cautious optimizers avoid this issue by adding a simple mask function based on the sign consistency of  $\mathbf{u}_t$  and  $\mathbf{w}_t$ :

$$\mathbf{w}_{t+1} \leftarrow \mathbf{w}_t - \epsilon_t \mathbf{u}_t \circ \phi(\mathbf{u}_t \circ \mathbf{g}_t),$$

where  $\circ$  denotes an element-wise product, and  $\phi$  is an element-wise map that reweights the update based on the product  $\mathbf{u}_t \circ \mathbf{g}_t$ . We simply take as  $\phi(x) = \mathbb{I}(x > 0)$  so that the update is zeroed out for coordinates on which the sign of  $\mathbf{u}_t$  and  $\mathbf{g}_t$  are inconsistent.

This modification ensures the new update to have a non-negative inner product with the gradient, and hence decreases the loss monotonically when the step size is sufficiently small. Specifically, Taylor approximation shows

$$\mathcal{L}(\mathbf{w}_{t+1}) - \mathcal{L}(\mathbf{w}_t) \approx \epsilon_t (\mathbf{u}_t \circ \mathbf{g}_t)^\top \phi(\mathbf{u}_t \circ \mathbf{g}_t) \leq 0.$$

This ensures decrease of the loss, i.e.,  $\mathcal{L}(\mathbf{w}_{t+1}) \leq \mathcal{L}(\mathbf{w}_t)$ , when the step size is sufficiently small.

In addition, we show in theoretical analysis that the modified algorithm converges to local optima under mild conditions of the based optimizers. An interesting aspect of this is that the algorithm would not stuck at non-stationary points of the loss, even if  $\mathbf{u}_t$  is completely conflicting with  $\mathbf{g}_t$ . This is because  $\mathbf{u}_t$  will be updated to eventually have a positive inner product with  $\mathbf{g}_t$  in valid momentum optimizers if it is stuck at a non-stationary point.

Theoretically, we show that the modified algorithm guarantees to converge to local optima for optimizers that admit a Hamiltonian+Descent structure (Chen et al., 2023a; Liang et al., 2024), which broadly includes almost all existing popular algorithms, including Adam, Lion, and heavy ball, and Nesterov momentum. For these algorithms, we show that the cautious optimizer with  $\phi$  satisfying  $x\phi(x) \geq \max(x, 0)$  retain the monotonic decreasing properties of the original Lyapunov (or Hamiltonian) functions of these algorithms, while in addition to also minimizing the loss function.

To summarize our contributions, we shall follow:

- We propose Cautious Optimizer, a simple performance boost of any momentum-based optimizers with one line of code.
- We show theoretically that cautious optimizers preserve the convergence guarantee of the base optimizer in addition to speeding up the decrease of the loss function.
- We show universal improvement by scaling LLaMA from 60M to 1B and pretraining MAE on ImageNet1K up to 1.47x faster.

---

**Algorithm 2** Cautious AdamW (C-AdamW)
 

---

**Require:** parameter  $\mathbf{w}$ , step sizes  $\{\epsilon_t\}$ , dampening factors  $\beta_1, \beta_2 \in [0, 1)$ ,  $\epsilon > 0$ , weight decay  $\gamma \geq 0$

```

1: Initialize  $t = 0$ ,  $\mathbf{m}_0 = \mathbf{v}_0 = \mathbf{0}$ 
2: while  $\mathbf{w}_t$  not converged do
3:    $t \leftarrow t + 1$ 
4:    $\mathbf{g}_t \leftarrow \nabla_{\mathbf{w}} \mathcal{L}_t(\mathbf{w}_{t-1})$ 
5:    $\mathbf{m}_t \leftarrow \beta_1 \mathbf{m}_{t-1} + (1 - \beta_1) \mathbf{g}_t$ 
6:    $\mathbf{v}_t \leftarrow \beta_2 \mathbf{v}_{t-1} + (1 - \beta_2) \mathbf{g}_t^2$ 
7:    $\hat{\mathbf{m}}_t \leftarrow \mathbf{m}_t / (1 - \beta_1^t)$ 
8:    $\hat{\mathbf{v}}_t \leftarrow \mathbf{v}_t / (1 - \beta_2^t)$ 
9:    $\mathbf{u}_t \leftarrow \hat{\mathbf{m}}_t / (\sqrt{\hat{\mathbf{v}}_t} + \epsilon)$ 
10:   $\phi_t \leftarrow \mathbb{I}(\mathbf{u}_t \circ \mathbf{g}_t \geq 0)$  // Compute alignment mask
11:   $\bar{\epsilon}_t = \epsilon_t \frac{d}{\|\phi_t\|_0 + 1}$  // Scale lr,  $d$  is dimension of  $\phi_t$ 
12:   $\mathbf{w}_t \leftarrow \mathbf{w}_{t-1} - \bar{\epsilon}_t \phi_t \circ \mathbf{u}_t$ 
13:   $\mathbf{w}_t \leftarrow \mathbf{w}_t - \bar{\epsilon}_t \gamma \mathbf{w}_t$  // Add weight decay
14: end while
    
```

---

## 2. Theory

We start with introducing a general Hamiltonian descent framework for the continuous-time forms of general momentum algorithms (Section 2.1). We then introduce the cautious optimizers in the continuous time form and discuss its theoretical properties (Section 2.2). Finally, we discuss in Section 2.3 theoretical properties of cautious optimizers in discrete time forms.

### 2.1. Hamiltonian+Descent

In the continuous-time form, most momentum-based algorithms can be viewed as a variant of the damped Hamiltonian system, which admits a Lyapunov (or Hamiltonian) function and their convergence towards the stationary points of the loss function. The Lyapunov function is an augmented loss function  $\mathcal{H}(\mathbf{w}, \mathbf{s})$  on both the weights  $\mathbf{w}$  and the momentum states  $\mathbf{s}$ , and should satisfy  $\min_{\mathbf{s}} \mathcal{H}(\mathbf{w}, \mathbf{s}) = \mathcal{L}(\mathbf{w})$ , so that minimizing  $\mathcal{L}(\mathbf{w})$  is equivalent to minimizing  $\mathcal{H}(\mathbf{w}, \mathbf{s})$ . This is achieved by is

$$\mathcal{H}(\mathbf{w}, \mathbf{s}) = \mathcal{L}(\mathbf{w}) + \mathcal{K}(\mathbf{s}),$$

where  $\mathcal{K}(\cdot)$  is any lower-bounded function. Physically, we can think  $\mathcal{H}$  as the total energy of a system parameterized by  $(\mathbf{w}, \mathbf{s})$ , and  $\mathcal{L}$  and  $\mathcal{K}$  as the potential energy and kinetic energy, respectively.

The continuous-time form of common momentum-based algorithms can be unified into

$$\begin{aligned} \frac{d}{dt} \mathbf{w}_t &= -\nabla \mathcal{K}(\mathbf{s}_t) - \Phi_t(\nabla \mathcal{L}(\mathbf{w}_t)) \\ \frac{d}{dt} \mathbf{s}_t &= \nabla \mathcal{L}(\mathbf{w}_t) - \Psi_t(\nabla \mathcal{K}(\mathbf{s}_t)), \end{aligned} \quad (1)$$

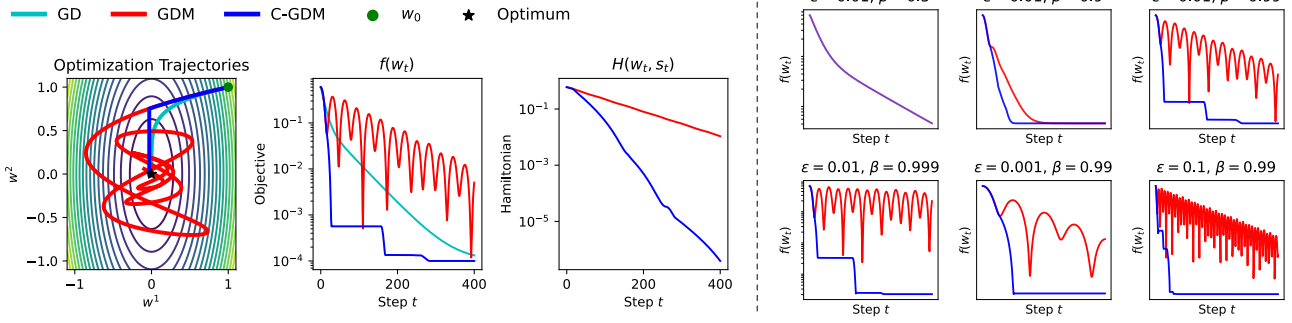


Figure 2: **Left:** We compare gradient descent with momentum (GDM) against its cautious variant (C-GDM) (we also provide gradient descent (GD) result as a baseline and use a 10x larger step size for GD than GDM and C-GDM). Details are provided in Section 3.1. The first plot shows the optimization trajectories from the two optimizers, where both optimizers start from (1, 1) with a zero-initialized momentum. C-GDM successfully lands at the optimum without overshooting. The second and third plots confirm that C-GDM always monotonically decreases both the objective and the Hamiltonian of the original GDM. **Right:** In this plot, we plot  $f(w_t)$  versus  $t$  for C-GDM and GDM with different combinations  $(\epsilon, \beta)$ . Across all combinations, C-GDM outperforms GDM.

where  $\Phi(\cdot), \Psi(\cdot)$  are two monotonic mappings satisfying

$$\|\mathbf{x}\|_{\Phi_t}^2 := \langle \mathbf{x}, \Phi_t(\mathbf{x}) \rangle \geq 0, \quad \|\mathbf{x}\|_{\Psi_t}^2 := \langle \mathbf{x}, \Psi_t(\mathbf{x}) \rangle \geq 0,$$

for any  $\mathbf{x}$ . With  $\Phi(\mathbf{x}) = \Psi(\mathbf{x}) = 0$ , the system in (9) reduces to the standard Hamiltonian system that keeps  $\mathcal{H}(\mathbf{w}_t, \mathbf{s}_t) = \text{const}$  along the trajectory. When adding the descending components with  $\Phi$  and  $\Psi$ , the system then keeps  $\mathcal{H}(\mathbf{w}, \mathbf{s})$  monotonically non-decreasing:

$$\frac{d}{dt} \mathcal{H}(\mathbf{w}_t, \mathbf{s}_t) = -\Delta_{\mathcal{H}}(\mathbf{w}_t, \mathbf{s}_t) \leq 0, \quad (2)$$

where

$$\Delta_{\mathcal{H}}(\mathbf{w}_t, \mathbf{s}_t) := \|\nabla \mathcal{L}(\mathbf{w}_t)\|_{\Phi_t}^2 + \|\nabla \mathcal{K}(\mathbf{s}_t)\|_{\Psi_t}^2.$$

On the other hand,  $\mathcal{L}(\mathbf{w})$ , which is the true objective, is not necessarily decreasing monotonically. There can be cases when  $\mathbf{w}$  increases temporarily, while the total energy  $\mathcal{H} = \mathcal{L} + \mathcal{K}$  remains decreasing. Specifically, we have

$$\frac{d}{dt} \mathcal{L}(\mathbf{w}_t) = -\Delta_{\mathcal{L}}(\mathbf{w}_t, \mathbf{s}_t), \quad (3)$$

where

$$\Delta_{\mathcal{L}}(\mathbf{w}_t, \mathbf{s}_t) := \nabla \mathcal{L}(\mathbf{w}_t)^\top \nabla \mathcal{K}(\mathbf{s}_t) + \|\nabla \mathcal{L}(\mathbf{w}_t)\|_{\Phi_t}^2.$$

$\Delta_{\mathcal{L}}(\mathbf{w}_t, \mathbf{s}_t)$  is not necessarily non-negative due to the cross term.

**Example 2.1.** Adam (Kingma, 2014) yields the following continuous-time form and Hamiltonian,

$$\begin{aligned} \frac{d}{dt} \mathbf{w}_t &= -\frac{\mathbf{m}_t}{\sqrt{\mathbf{v}_t + \epsilon}}, & \frac{d}{dt} \mathbf{m}_t &= a(\nabla \mathcal{L}(\mathbf{w}_t) - \mathbf{m}_t), \\ & & \frac{d}{dt} \mathbf{v}_t &= b(\nabla \mathcal{L}(\mathbf{w}_t)^{\odot 2} - \mathbf{v}_t) \end{aligned}$$

$$\text{with} \quad \mathcal{H}(\mathbf{w}, \mathbf{m}, \mathbf{v}) = \mathcal{L}(\mathbf{w}) + \frac{1}{2a} \left\langle \frac{\mathbf{m}}{\sqrt{\mathbf{v} + \epsilon}}, \mathbf{m} \right\rangle.$$

We can show that  $\frac{d}{dt} \mathcal{H}(\mathbf{w}_t, \mathbf{m}_t, \mathbf{v}_t) \leq 0$  when  $a \geq b/4$ .

**Example 2.2.** The Lion-K optimizer (Chen et al., 2023b;a) (without weight decay) can be written into

$$\begin{aligned} \frac{d}{dt} \mathbf{w}_t &= \nabla \mathcal{K}((1-b)\mathbf{m}_t - b\nabla \mathcal{L}(\mathbf{w}_t)), \\ \frac{d}{dt} \mathbf{m}_t &= -a(\nabla \mathcal{L}(\mathbf{w}_t) + \mathbf{m}_t) \end{aligned}$$

where  $a \geq 0, b \in [0, 1]$  and  $\mathcal{K}(\mathbf{x})$  is any convex function that attains the minimum at  $\mathbf{x} = 0$ . One of its Hamiltonians that yields the Hamiltonian+descent structure (Eq (13) in Chen et al. (Chen et al., 2023a)) is

$$\mathcal{H}(\mathbf{w}, \mathbf{m}) = a\mathcal{L}(\mathbf{w}) + \frac{1}{1-b} \mathcal{K}((1-b)\mathbf{m}).$$

See (Chen et al., 2023a) for other Hamiltonian functions. Lion-K includes a large family algorithms as special cases, including Polyka momentum, Nesterov momentum, signed momentum, mirror descent, Frank-Wolfe, etc.

## 2.2. Cautious Dynamics

Our idea is to change the dynamics to make it *simultaneously* decrease both  $\mathcal{H}(\mathbf{w}, \mathbf{s})$  and  $\mathcal{L}(\mathbf{w})$ . We do this with a modified system:

$$\begin{aligned} \bar{\mathbf{x}}_t &= \nabla \mathcal{L}(\bar{\mathbf{w}}_t) \circ \nabla \mathcal{K}(\bar{\mathbf{s}}_t) \\ \frac{d}{dt} \bar{\mathbf{w}}_t &= -\phi(\bar{\mathbf{x}}_t) \circ \nabla \mathcal{K}(\bar{\mathbf{s}}_t) - \Phi_t(\nabla \mathcal{L}(\bar{\mathbf{w}}_t)) \\ \frac{d}{dt} \bar{\mathbf{s}}_t &= \nabla \mathcal{L}(\bar{\mathbf{w}}_t) - \Psi_t(\nabla \mathcal{K}(\bar{\mathbf{s}}_t)), \end{aligned} \quad (4)$$

where  $\circ$  denotes the element-wise product and  $\phi$  is a vector to vector mapping. Here we weigh each element of the

update direction of  $W_t$  based on the product of  $\nabla\mathcal{L}(\mathbf{w})$  and  $\nabla\mathcal{K}(\mathbf{s})$ . The following conditions on the choice of function  $\phi$  ensure that the system simultaneously decreases both  $\mathcal{H}$  and  $L$  simultaneously.

**Theorem 2.3.** *Following the dynamics in (10), we have*

$$\frac{d}{dt}\mathcal{H}(\bar{\mathbf{w}}_t, \bar{\mathbf{s}}_t) = (\bar{\mathbf{x}}_t^\top(\mathbf{1} - \phi(\bar{\mathbf{x}}_t)) - \Delta_{\mathcal{H}_t}(\bar{\mathbf{w}}_t, \bar{\mathbf{s}}_t)),$$

and

$$\begin{aligned} \frac{d}{dt}\mathcal{L}(\bar{\mathbf{w}}_t) &= -\bar{\mathbf{x}}_t^\top\phi(\bar{\mathbf{x}}_t) - \|\nabla\mathcal{L}(\bar{\mathbf{w}}_t)\|_{\Phi_t}^2 \\ &= (\bar{\mathbf{x}}_t^\top(\mathbf{1} - \phi(\bar{\mathbf{x}}_t)) - \Delta_{\mathcal{L}_t}(\bar{\mathbf{w}}_t, \bar{\mathbf{s}}_t)), \end{aligned}$$

Here,  $\Delta_{\mathcal{H}_t}(\bar{\mathbf{w}}_t, \bar{\mathbf{s}}_t)$  and  $\Delta_{\mathcal{L}_t}(\bar{\mathbf{w}}_t, \bar{\mathbf{s}}_t)$ , as defined in (2) and (3), respectively, represent the decreasing rates of  $\mathcal{H}$  and  $\mathcal{L}$  in accordance with the original system (9). Hence:

- If  $\mathbf{x}^\top(\mathbf{1} - \phi(\mathbf{x})) \leq 0$  for  $\forall \mathbf{x}$ , then both  $\mathcal{H}$  and  $\mathcal{L}$  decreases faster than the original system:

$$\begin{aligned} \frac{d}{dt}\mathcal{H}(\bar{\mathbf{w}}_t, \bar{\mathbf{s}}_t) &\leq -\Delta_{\mathcal{H}_t}(\bar{\mathbf{w}}_t, \bar{\mathbf{s}}_t) \leq 0, \\ \frac{d}{dt}\mathcal{L}(\bar{\mathbf{w}}_t) &\leq -\Delta_{\mathcal{L}_t}(\bar{\mathbf{w}}_t, \bar{\mathbf{s}}_t). \end{aligned}$$

- If  $\mathbf{x}^\top\phi(\mathbf{x}) \geq 0$  for  $\forall \mathbf{x}$ , then  $\mathcal{L}$  decreases monotonically,

$$\frac{d}{dt}\mathcal{L}(\bar{\mathbf{w}}_t) \leq 0.$$

*Proof.* See Appendix.  $\square$

If  $\phi$  is an element-wise mapping, then  $\phi$  satisfies both conditions if

$$x\phi(x) \geq \max(x, 0), \quad \forall x \in \mathbb{R}. \quad (5)$$

In this case, both  $\mathcal{H}$  and  $L$  decrease monotonically following the cautious dynamics, with a rate faster than the original systems. We recommend the default choice of  $\phi(x) = \mathbb{I}(x \geq 0)$ , which satisfies both conditions while being the closest to a constant function.

**Corollary 2.4.** *Assume that the norm  $\|\cdot\|_{\Psi}^2$  is positive definite,  $\Psi(0) = 0$ , and that  $H(\mathbf{w}, \mathbf{s}) = \mathcal{L}(\mathbf{w}) + \kappa(\mathbf{s})$  is differentiable. Then, the bounded solutions of the original system (9) converge to a stationary point of  $H(\mathbf{w}, \mathbf{s})$ . Similarly, the bounded solutions of (10) also converge to a stationary point of  $H(\mathbf{w}, \mathbf{s})$ .*

*Proof.* See Appendix A.  $\square$

### 2.3. Discrete-Time Analysis

We provide analysis for the discrete time, showing that cautious optimizers can only be better than the original optimizers under mild conditions.

We will consider a generic update of form

$$\begin{aligned} \mathbf{w}_{k+1} &= \mathbf{w}_k - \epsilon_k \mathbf{u}_k(\mathbf{w}_k, \mathbf{s}_k), \\ \mathbf{s}_{k+1} &= \mathbf{s}_k + \mathbf{v}_k(\mathbf{w}_k, \mathbf{s}_k), \end{aligned} \quad (6)$$

where  $\mathbf{u}_k, \mathbf{v}_k$  are vector fields that define the updates. and  $\epsilon_k$  is the step size. and its cautious variant:

$$\bar{\mathbf{u}}_k = \mathbf{u}_k(\bar{\mathbf{w}}_k, \bar{\mathbf{s}}_k) \quad (7)$$

$$\bar{\mathbf{w}}_{k+1} = \bar{\mathbf{w}}_k - \epsilon_k \bar{\mathbf{u}}_k \circ \bar{\phi}_k$$

$$\bar{\mathbf{s}}_{k+1} = \bar{\mathbf{s}}_k + \mathbf{v}_k(\bar{\mathbf{w}}_k, \bar{\mathbf{s}}_k), \quad (8)$$

where  $\bar{\phi}_k$  is a mask vector determined by the algorithm. Our analysis will consider both the element-wise mask  $\bar{\phi}_k = \mathbb{I}(\bar{\mathbf{u}}_k \circ \bar{\mathbf{g}}_k > 0)$ , and inner product mask,  $\bar{\phi}_k = \mathbb{I}(\bar{\mathbf{u}}_k^\top \bar{\mathbf{g}}_k > 0)$ , where  $\bar{\mathbf{g}}_k = \nabla\mathcal{L}(\bar{\mathbf{w}}_k)$ . The difference is that the inner product mask is scalar and masks the update vector as a whole, while element-wise mask treat each element separately.

**Inner Product Mask for Convex Losses** We start with the case of using inner product masks on convex loss functions. This case is interesting because the cautious optimizers is always no worse than the base optimizers, *regardless of the step size choices.*

**Theorem 2.5.** *Assume  $\mathcal{L}(\cdot)$  is convex, and  $\bar{\phi}_k = \mathbb{I}(\bar{\mathbf{u}}_k^\top \nabla\mathcal{L}(\bar{\mathbf{w}}_k) \geq 0)$ . Then, starting from  $(\mathbf{w}_k, \mathbf{s}_k) = (\bar{\mathbf{w}}_k, \bar{\mathbf{s}}_k)$ , we have*

$$\mathcal{L}(\bar{\mathbf{w}}_{k+1}) \leq \mathcal{L}(\mathbf{w}_{k+1}).$$

which holds for any step size  $\epsilon_k \geq 0$ .

*Proof.* If  $\bar{\mathbf{u}}_k^\top \nabla\mathcal{L}(\bar{\mathbf{w}}_k) \geq 0$ , we have  $\bar{\phi}_k = 1$ , and  $\mathbf{w}_{k+1} = \bar{\mathbf{w}}_{k+1}$ , and  $\mathcal{L}(\bar{\mathbf{w}}_{k+1}) = \mathcal{L}(\mathbf{w}_{k+1})$ .

If  $\bar{\mathbf{u}}_k^\top \nabla\mathcal{L}(\bar{\mathbf{w}}_k) < 0$ , we have  $\bar{\mathbf{w}}_{k+1} = \mathbf{w}_k$ , and by the convexity of  $\mathcal{L}$ :

$$\begin{aligned} \mathcal{L}(\mathbf{w}_{k+1}) - \mathcal{L}(\bar{\mathbf{w}}_{k+1}) &= \mathcal{L}(\mathbf{w}_k - \epsilon_k \bar{\mathbf{u}}_k) - \mathcal{L}(\mathbf{w}_k) \\ &\geq -\epsilon_k \bar{\mathbf{u}}_k^\top \nabla\mathcal{L}(\mathbf{w}_k) > 0. \end{aligned}$$

This proves the result.  $\square$

**Corollary 2.6.** *Consider the elementary test function:*

$$\mathcal{L}(\mathbf{w}) = \frac{1}{2} \|\mathbf{a} \circ \mathbf{w}\|_2^2.$$

where  $\mathbf{a}$  is a non-zero vector. Assume  $\mathbf{u}_k$  and  $\mathbf{v}_k$  are element-wise mappings. We have  $\mathcal{L}(\bar{\mathbf{w}}_{k+1}) \leq \mathcal{L}(\mathbf{w}_{k+1})$  given  $(\mathbf{w}_k, \mathbf{s}_k) = (\bar{\mathbf{w}}_k, \bar{\mathbf{s}}_k)$ , with either the inner product mask  $\bar{\phi}_k = \mathbb{I}(\bar{\mathbf{u}}_k^\top \nabla\mathcal{L}(\bar{\mathbf{w}}_k) \geq 0)$ , or the element-wise mask  $\bar{\phi}_k = \mathbb{I}(\bar{\mathbf{u}}_k \circ \nabla\mathcal{L}(\bar{\mathbf{w}}_k) \geq 0)$ .

*Proof.* The inner product case is implied by Theorem 2.3. For element-wise mask, since the loss is an element-wise sum, and the update functions are element-wise mappings, which can apply Theorem 2.3 on each element.  $\square$

**Example: Local vs. Global Comparisons in a Quadratic Toy Model** Consider the objective function:  $\mathcal{L}(\mathbf{w}) = w_1^2 + \kappa w_2^2$ , where  $\kappa$  is the condition number. The optimal momentum convergence rate for this function is:  $\frac{\sqrt{\kappa}-1}{\sqrt{\kappa}+1}$ , as shown in (Goh, 2017). Setting  $\kappa = 4$ , we plot the convergence rate heatmap over  $(\alpha, \beta)$ -space, where  $\alpha$  and  $\beta$  are the learning rate and momentum parameters.

The heat-map shows that the cautious method achieves a lower optimal convergence rate than the momentum method, highlighted by the red dot in Figure 3.

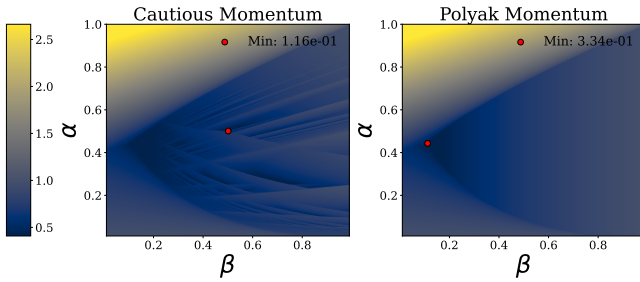


Figure 3: Convergence rate heatmaps for  $\kappa = 4$ . Left: Cautious method; Right: Momentum method. Red dots highlight the optimal (minimal) convergence rate for each method.

**General Cases** We now consider element-wise masks with general loss functions, in which case we need to impose assumptions on step sizes.

**Remark** Assume that the loss function  $\mathcal{L}(\cdot)$  is convex and element-wise separable, i.e.,  $\mathcal{L}(\mathbf{w}) = \sum_i \mathcal{L}_i(w_i)$ , where each  $\mathcal{L}_i$  is a convex function. Additionally, let  $\bar{\phi}_k = \mathbb{I}(\bar{\mathbf{u}}_k \circ \nabla \mathcal{L}(\bar{\mathbf{w}}_k) \geq 0)$ , where  $\mathbb{I}(\cdot)$  denotes the element-wise indicator function and  $\circ$  represents the element-wise product.

Under these conditions, starting from  $(\mathbf{w}_k, \mathbf{s}_k) = (\bar{\mathbf{w}}_k, \bar{\mathbf{s}}_k)$ , for any step size  $\epsilon_k \geq 0$ , we have  $\mathcal{L}(\mathbf{w}_{k+1}) \leq \mathcal{L}(\bar{\mathbf{w}}_{k+1})$ .

**Theorem 2.7.** Assuming  $\mathcal{L}(\cdot)$  is  $\mu$ -smooth, and

$$\bar{\phi}_k = \mathbb{I}(\nabla \mathcal{L}(\bar{\mathbf{w}}_k)^\top \bar{\mathbf{u}}_k \geq -\frac{\mu \epsilon_k}{2} \|\bar{\mathbf{u}}_k\|^2).$$

Then, starting from  $(\mathbf{w}_k, \mathbf{s}_k) = (\bar{\mathbf{w}}_k, \bar{\mathbf{s}}_k)$ , we have

$$\mathcal{L}(\bar{\mathbf{w}}_{k+1}) \leq \mathcal{L}(\mathbf{w}_{k+1}).$$

which holds for any step size  $\epsilon_k \geq 0$ .

**Theorem 2.8** (Larger Loss Decreasing). Assume loss function  $\mathcal{L}(\cdot)$  is differentiable and  $\mu$ -smooth, element-wise operator  $\phi$  satisfies (5), and  $\bar{\phi}_k = \phi(\nabla \mathcal{L}(\bar{\mathbf{w}}_k) \circ \bar{\mathbf{u}}_k)$ . Then,

starting from  $(\mathbf{w}_k, \mathbf{s}_k) = (\bar{\mathbf{w}}_k, \bar{\mathbf{s}}_k)$ , we have

$$\mathcal{L}(\bar{\mathbf{w}}_{k+1}) \leq \mathcal{L}(\mathbf{w}_{k+1}).$$

which holds for step size  $\epsilon_k \leq \frac{2\mathbf{x}_k^\top (\mathbf{1} - \phi(\mathbf{x}_k))}{\|\mathcal{R}_k\| (2\mu \|\mathbf{u}_k\| + \|\mathcal{R}_k\|)}$ , where  $\mathcal{R}_k = \mathbf{u}_k \circ (\mathbf{1} - \mathcal{M})$ .

### 3. Experiments

In this section, we evaluate the performance of cautious optimizers compared to their standard counterparts, highlighting the benefits introduced by the cautious masking mechanism. We begin with a 2D toy experiment to provide a visual demonstration of how cautious masking improves optimization. Subsequently, we extend the evaluation to large-scale pretraining tasks for both language and vision models, comparing the performance of standard optimizers and their cautious variants.

#### 3.1. 2D Optimization Toy

We consider a 2D optimization problem, where the decision variable  $\mathbf{w} = (w^1, w^2) \in \mathbb{R}^2$ . The objective is  $f(\mathbf{w}) = 0.5(w^1)^2 + 0.1(w^2)^2$ . Apparently the optimum is at  $\mathbf{w}^* = (0, 0)$ . We apply gradient descent (GD), gradient descent with momentum (GDM), and cautious gradient descent with momentum (C-GDM) on this toy example, starting from  $\mathbf{w}_0 = (1, 1)$ . Specifically, for GDM, we adopt the conventional momentum update:

$$\begin{aligned} \mathbf{s}_t &\leftarrow \beta \mathbf{s}_{t-1} + \nabla f(\mathbf{w}_t), \\ \mathbf{w}_t &\leftarrow \mathbf{w}_{t-1} - \epsilon \mathbf{s}_t, \end{aligned}$$

where  $\beta \in [0, 1)$  is the dampening factor, and  $\epsilon$  is a constant learning rate. When using  $\beta = 0.99$  and  $\epsilon = 0.01$  for GDM and C-GDM,  $\epsilon = 0.1$  for GD, the results are visualized in Figure 2.

**Observation:** From the left of Figure 2, one can see that GDM, due to the momentum, has fluctuating  $f(w_t)$ , while C-GDM ensures that  $f(w_t)$  monotonically decreases. In addition, C-GDM achieves a faster drop in terms of GDM's Hamiltonian. On the right of Figure 2, we ablate over different combinations of  $(\beta, \epsilon) \in \{(0.01, 0.5), (0.01, 0.9), (0.01, 0.99), (0.01, 0.999), (0.1, 0.99), (0.001, 0.99)\}$ . Across all settings, C-GDM outperforms GDM, confirming the importance of cautious masking.

#### 3.2. Pretraining Large Language Models (LLMs)

We begin by investigating the language modeling task using the LLaMA (Touvron et al., 2023) model as the foundational architecture. Variants of LLaMA with parameter sizes ranging from 60M to 1B (specifically 60M, 100M, 350M, and 1B) are considered in this study. The models are trained on the C4 (Colossal Clean Crawled Corpus) dataset (Raffel

# Params	Perplexity ( $\downarrow$ )			
	AdamW	C-AdamW	Lion	C-Lion
60M	31.17	<b>30.78</b>	55.17	<b>40.04</b>
100M	26.96	<b>26.82</b>	41.69	<b>33.21</b>
350M	22.58	<b>22.14</b>	29.10	<b>22.84</b>
1B	24.02	<b>22.00</b>	22.00	<b>21.17</b>

Table 1: To demonstrate scaling law (Kaplan et al., 2020), eval perplexity for LLaMA models pretrained on C4 for 10K steps. Cautious Optimizer is better across all model sizes. Lower perplexity is better. Hyperparameters can be found in appendix.

et al., 2020), a large-scale web-crawled text corpus containing billions of tokens.

The extensive scale of the C4 dataset, coupled with the complexity of the LLaMA architecture, results in prolonged training durations, often spanning weeks or months. For optimization, we employ AdamW (Loshchilov, 2017) and Lion (Chen et al., 2023c), two widely used optimizers in modern language modeling, as baselines. These are compared with their cautious counterparts, which we term Cautious AdamW (C-AdamW) and Cautious Lion (C-Lion). Figure 4 illustrates the training curves of LLaMA-1B for AdamW, C-AdamW, Lion, and C-Lion. Validation perplexities for all model sizes (60M, 100M, 350M, and 1B) across the four optimizers are summarized in Table 1. The complete hyperparameter configurations for language model training are detailed in Table 4 in the Appendix.

**Observation:** As shown in Figure 4, C-AdamW and C-Lion demonstrate significant improvements in sample efficiency, achieving a **1.47x** and **1.28x** gain over AdamW and Lion, respectively, on the LLaMA-1B model. Notably, these improvements require only a single additional line of code and incur no extra computational overhead. On the other hand, we observe an interesting phenomenon that the gap between C-AdamW and AdamW increases as model size increases, but for Lion it is the reversed. Quantatively, Table 1 reveals that the cautious optimizers consistently outperform their standard counterparts across all model sizes.

To further assess the quality of models trained with cautious optimizers, we conduct downstream evaluations on the GLUE benchmark (Wang, 2018), a widely used suite for evaluating pretrained language models. GLUE comprises nine diverse natural language understanding tasks, including sentence similarity, text classification, entailment, and question answering, as well as a diagnostic dataset for fine-grained linguistic analysis. We focus on six tasks—Microsoft Research Paraphrase Corpus (MRPC), Recognizing Textual Entailment (RTE), Stanford Sentiment Treebank (SST-2), Multi-Genre Natural Language Inference (MNLI), Question Natural Language Inference (QNLI), and

Quora Question Pairs (QQP)—which do not require additional fine-tuning for evaluation. Table 2 summarizes the downstream performance of models pretrained using AdamW and C-AdamW on these six tasks, alongside their average score, which serves as an overall performance metric.

**Observation:** As shown in Table 2, models trained with C-AdamW not only achieve lower training and validation perplexities but also deliver a notable **2%** improvement in downstream scores, demonstrating the practical advantages of cautious optimization.

### 3.3. Pretraining Masked Autoencoders (MAEs)

Masked Autoencoders (MAEs) (He et al., 2022) have emerged as a powerful approach for pretraining Vision Transformers (ViTs) (Dosovitskiy, 2020) on large-scale datasets like ImageNet-1K (Russakovsky et al., 2015). This task involves reconstructing 75% of randomly masked image patches, a challenging objective that requires extensive training over hundreds of epochs and millions of images. The primary goal is to learn robust visual representations that are generalizable across downstream vision tasks. The quality of these representations is typically measured by the final evaluation loss, which reflects how accurately the model reconstructs masked test images; lower evaluation loss indicates higher-quality representations. The results of our experiments are summarized in Figure 3, where we compare the performance of the Cautious Optimizer against the AdamW baseline.

**Observation:** From Table 3, we observe that the Cautious Optimizer achieves a consistently lower final evaluation loss compared to AdamW. This result highlights the effectiveness of the cautious approach in improving the precision of reconstruction and, consequently, the quality of the learned visual representations.

## 4. Related Work

In this section, we provide a brief overview of existing efforts on designing Adam-like optimizers, and the related works on Hamiltonian dynamics.

**Adam and Its Variants** There exist a long series of works on variants of Adam (Kingma, 2014; Loshchilov & Hutter, 2017). AdaFactor (Shazeer & Stern, 2018) factorizes the second order momentum. AdamW (Loshchilov & Hutter, 2017) proposed a simple modification to recover the original formulation of weight decay regularization by *decoupling* the weight decay from the optimization steps taken w.r.t. the loss function. NAdam (Dozat, 2016) proposes to combine Nesterov update with Adam. AdaBelief (Zhuang et al., 2020) changes the second momentum  $v_t$  from the EMA of

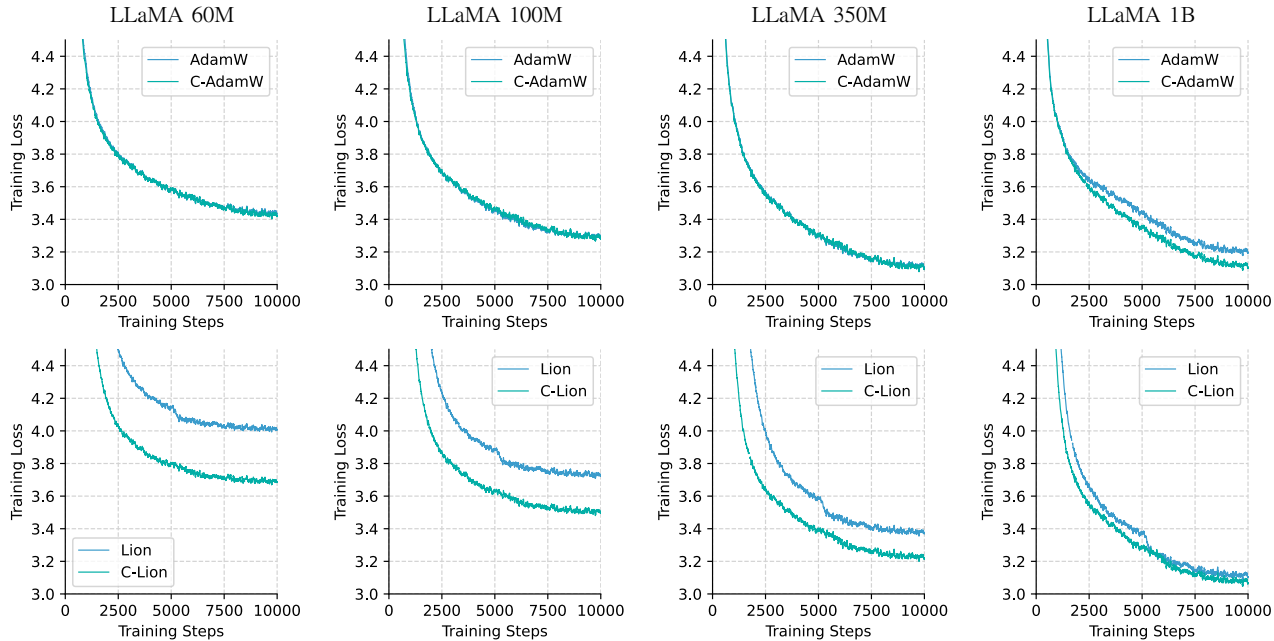


Figure 4: Training loss curves for AdamW, C-AdamW, Lion, C-Lion on LLaMA with 60M, 100M, 350M, and 1B parameters.

Method	MRPC	RTE	SST2	MNLI	QNLI	QQP	AVG (↑)
AdamW	67.2	52.0	49.1	32.9	49.5	36.8	47.9
C-AdamW	68.4	46.6	63.0	32.7	49.5	36.8	<b>49.5</b>

Table 2: Standardized GLUE evaluation for 1B model checkpoints using eval-harness. Results are reported for various downstream tasks.

Method	Final Eval Loss (↓)
AdamW	0.6085
C-AdamW	<b>0.5926</b>

Table 3: Evaluation loss of pretrained MAEs on ImageNet1K on ViT backbone for 50 epochs, using AdamW and C-AdamW.

$g_t^2$  to the EMA of  $(g_t - m_t)^2$ . Adan (Xie et al., 2024) introduced an extra momentum term to improve training but with extra memory cost. More recently, ADOPT (Taniguchi et al., 2024) folds normalized updates into first order momentum updates. Our propose C-AdamW is a single-line modification based on AdamW, which is the most commonly used optimizer in large-model training nowadays. Different from the above work that focuses on making specific change to the Adam optimizer, our proposed solution works in general for all momentum-based optimizers.

**Hamiltonian Dynamics** Hamiltonian dynamics, also known as Hamiltonian mechanics or Hamiltonian formalism, is a mathematical framework used to describe the mo-

tion of particles and systems in classical mechanics (Abraham & Marsden, 2008). In the field of sampling, Hamiltonian Monte Carlo and its variants can traverse the optimization landscape more efficiently by combining the principles of Hamiltonian dynamics with Markov Chain Monte Carlo (MCMC) methods (Neal et al., 2011; Betancourt & Girolami, 2015; Hoffman & Gelman, 2014) Analyzing momentum-based algorithms (Sutskever et al., 2013; Nesterov, 1983) poses a unique challenge, given that the objective function doesn’t exhibit the monotonic decrease found in Gradient Descent (GD)(Jin et al., 2018). To address this in the convex setting, researchers have introduced multiple Lyapunov functions (Krichene et al., 2015; Wilson et al., 2016). (Jin et al., 2018) introduced Hamiltonian to get a convergence rate of stationary points.(Sutskever et al., 2013) led to physical interpretation of momentum (Sutskever et al., 2013) and Nesterov’s and Polyak’s methods (Nesterov, 1983). Recently, the Hamiltonian dynamics have been adopted for proving convergence rate for the Lion optimizer (Chen et al., 2023a) and its distributed variant (Liu et al., 2024).

## 5. Conclusion and Limitation

In summary, we introduce Cautious Optimizer, a straightforward enhancement for momentum-based optimizers that can be implemented with a single line of code. Our theoretical analysis demonstrates that the Cautious Optimizer not only preserves the convergence guarantees of the base optimizer but also accelerates the reduction of the loss function. Empirically, it delivers universal performance improvements, as evidenced by scaling Llama models from 60M to 1B parameters and achieving up to  $1.47 \times$  faster pretraining of MAE on ImageNet1K.

For future research, we provide a few promising directions: (1) Different  $\phi$  functions (2) Applying masking in eigenspace instead of parameter space (3) More rigorous analysis beyond convex cases. We hope that our work provides a strong foundation for exploring these directions.

**Limitations:** Our evaluation of this method remains preliminary due to limited computational resources. Despite early promising results, it remains uncertain whether Cautious Optimizers will deliver the anticipated improvements in broader applications and large-scale experiments.

## References

- Abraham, R. and Marsden, J. E. *Foundations of mechanics*. Number 364. American Mathematical Soc., 2008.
- Achiam, J., Adler, S., Agarwal, S., Ahmad, L., Akkaya, I., Aleman, F. L., Almeida, D., Altenschmidt, J., Altman, S., Anadkat, S., et al. Gpt-4 technical report. *arXiv preprint arXiv:2303.08774*, 2023.
- Bernstein, J., Wang, Y.-X., Azizzadenesheli, K., and Anandkumar, A. signsgd: Compressed optimisation for non-convex problems. In *International Conference on Machine Learning*, pp. 560–569. PMLR, 2018.
- Betancourt, M. and Girolami, M. Hamiltonian monte carlo for hierarchical models. *Current trends in Bayesian methodology with applications*, 79(30):2–4, 2015.
- Chen, L., Liu, B., Liang, K., and Liu, Q. Lion secretly solves constrained optimization: As lyapunov predicts. *arXiv preprint arXiv:2310.05898*, 2023a.
- Chen, X., Liang, C., Huang, D., Real, E., Wang, K., Liu, Y., Pham, H., Dong, X., Luong, T., Hsieh, C.-J., et al. Symbolic discovery of optimization algorithms. *arXiv preprint arXiv:2302.06675*, 2023b.
- Chen, X., Liang, C., Huang, D., Real, E., Wang, K., Liu, Y., Pham, H., Dong, X., Luong, T., Hsieh, C.-J., et al. Symbolic discovery of optimization algorithms. *arXiv preprint arXiv:2302.06675*, 2023c.
- Chen, X., Liang, C., Huang, D., Real, E., Wang, K., Pham, H., Dong, X., Luong, T., Hsieh, C.-J., Lu, Y., et al. Symbolic discovery of optimization algorithms. *Advances in neural information processing systems*, 36, 2024.
- Defazio, A., Yang, X. A., Mehta, H., Mishchenko, K., Khaled, A., and Cutkosky, A. The road less scheduled. *arXiv preprint arXiv:2405.15682*, 2024.
- Dosovitskiy, A. An image is worth 16x16 words: Transformers for image recognition at scale. *arXiv preprint arXiv:2010.11929*, 2020.
- Dozat, T. Incorporating nesterov momentum into adam. 2016.
- Goh, G. Why momentum really works. *Distill*, 2017. doi: 10.23915/distill.00006. URL <http://distill.pub/2017/momentum>.
- Gupta, V., Koren, T., and Singer, Y. Shampoo: Pre-conditioned stochastic tensor optimization. In *International Conference on Machine Learning*, pp. 1842–1850. PMLR, 2018.
- He, K., Chen, X., Xie, S., Li, Y., Dollár, P., and Girshick, R. Masked autoencoders are scalable vision learners. In *Proceedings of the IEEE/CVF conference on computer vision and pattern recognition*, pp. 16000–16009, 2022.
- Hoffman, M. D. and Gelman, A. The no-u-turn sampler: Adaptively setting path lengths in hamiltonian monte carlo. *Journal of Machine Learning Research*, 15(47):1593–1623, 2014. URL <http://jmlr.org/papers/v15/hoffman14a.html>.
- Jin, C., Netrapalli, P., and Jordan, M. I. Accelerated gradient descent escapes saddle points faster than gradient descent. In *Conference On Learning Theory*, pp. 1042–1085. PMLR, 2018.
- Kaplan, J., McCandlish, S., Henighan, T., Brown, T. B., Chess, B., Child, R., Gray, S., Radford, A., Wu, J., and Amodei, D. Scaling laws for neural language models. *arXiv preprint arXiv:2001.08361*, 2020.
- Kingma, D. P. Adam: A method for stochastic optimization. *arXiv preprint arXiv:1412.6980*, 2014.
- Krichene, W., Bayen, A., and Bartlett, P. L. Accelerated mirror descent in continuous and discrete time. *Advances in neural information processing systems*, 28, 2015.
- Liang, K., Liu, B., Chen, L., and Liu, Q. Memory-efficient llm training with online subspace descent. *arXiv preprint arXiv:2408.12857*, 2024.



- Liu, B., Wu, L., Chen, L., Liang, K., Zhu, J., Liang, C., Krishnamoorthi, R., and Liu, Q. Communication efficient distributed training with distributed lion. *arXiv preprint arXiv:2404.00438*, 2024.
- Loshchilov, I. Decoupled weight decay regularization. *arXiv preprint arXiv:1711.05101*, 2017.
- Loshchilov, I. and Hutter, F. Decoupled weight decay regularization. *arXiv preprint arXiv:1711.05101*, 2017.
- Loshchilov, I., Hutter, F., et al. Fixing weight decay regularization in adam. *arXiv preprint arXiv:1711.05101*, 5, 2017.
- Neal, R. M. et al. Mcmc using hamiltonian dynamics. *Handbook of markov chain monte carlo*, 2(11):2, 2011.
- Nesterov, Y. E. A method for solving the convex programming problem with convergence rate  $o(1/\kappa^2)$ . In *Dokl. akad. nauk Sssr*, volume 269, pp. 543–547, 1983.
- Raffel, C., Shazeer, N., Roberts, A., Lee, K., Narang, S., Matena, M., Zhou, Y., Li, W., and Liu, P. J. Exploring the limits of transfer learning with a unified text-to-text transformer. *Journal of machine learning research*, 21(140):1–67, 2020.
- Rombach, R., Blattmann, A., Lorenz, D., Esser, P., and Ommer, B. High-resolution image synthesis with latent diffusion models. In *Proceedings of the IEEE/CVF conference on computer vision and pattern recognition*, pp. 10684–10695, 2022.
- Russakovsky, O., Deng, J., Su, H., Krause, J., Satheesh, S., Ma, S., Huang, Z., Karpathy, A., Khosla, A., Bernstein, M., et al. Imagenet large scale visual recognition challenge. *International journal of computer vision*, 115: 211–252, 2015.
- Shazeer, N. and Stern, M. Adafactor: Adaptive learning rates with sublinear memory cost. In *International Conference on Machine Learning*, pp. 4596–4604. PMLR, 2018.
- Sutskever, I., Martens, J., Dahl, G., and Hinton, G. On the importance of initialization and momentum in deep learning. In *International conference on machine learning*, pp. 1139–1147. PMLR, 2013.
- Taniguchi, S., Harada, K., Minegishi, G., Oshima, Y., Jeong, S. C., Nagahara, G., Iiyama, T., Suzuki, M., Iwasawa, Y., and Matsuo, Y. Adopt: Modified adam can converge with any  $\beta_2$  with the optimal rate. *arXiv preprint arXiv:2411.02853*, 2024.
- Touvron, H., Lavril, T., Izacard, G., Martinet, X., Lachaux, M.-A., Lacroix, T., Rozière, B., Goyal, N., Hambro, E., Azhar, F., et al. Llama: Open and efficient foundation language models. *arXiv preprint arXiv:2302.13971*, 2023.
- Vyas, N., Morwani, D., Zhao, R., Shapira, I., Brandfonbrener, D., Janson, L., and Kakade, S. Soap: Improving and stabilizing shampoo using adam. *arXiv preprint arXiv:2409.11321*, 2024.
- Wang, A. Glue: A multi-task benchmark and analysis platform for natural language understanding. *arXiv preprint arXiv:1804.07461*, 2018.
- Wilson, A. C., Recht, B., and Jordan, M. I. A lyapunov analysis of momentum methods in optimization. *arXiv preprint arXiv:1611.02635*, 2016.
- Xie, X., Zhou, P., Li, H., Lin, Z., and Yan, S. Adan: Adaptive nesterov momentum algorithm for faster optimizing deep models. *IEEE Transactions on Pattern Analysis and Machine Intelligence*, 2024.
- Zhang, G., Kenta, N., and Kleijn, W. B. Extending adamw by leveraging its second moment and magnitude. *arXiv preprint arXiv:2112.06125*, 2021.
- Zhuang, J., Tang, T., Ding, Y., Tatikonda, S. C., Dvornek, N., Papademetris, X., and Duncan, J. Adabelief optimizer: Adapting stepsizes by the belief in observed gradients. *Advances in neural information processing systems*, 33: 18795–18806, 2020.

## A. Appendix

### A.1. Hamiltonian + Descent

Momentum-based algorithms can be typically viewed as monotonic descending algorithms on an augmented loss  $H(W, S)$ , which satisfies  $\min_S H(W, S) = \mathcal{L}(W)$ , so that minimizing  $\mathcal{L}(W)$  is equivalent to minimizing  $H(W, S)$ . A typical choice is

$$H(\mathbf{w}, \mathbf{s}) = \mathcal{L}(\mathbf{w}) + \mathcal{K}(\mathbf{s}),$$

where  $\mathcal{K}(\cdot)$  is any lower bounded function. We may refer  $H(\mathbf{w}, \mathbf{s})$  as a Hamiltonian function. Physically, one can show  $\mathcal{L}(\mathbf{w})$  and  $\mathcal{K}(\mathbf{s})$  the potential energy and kinetic energy, respectively.

The continuous-time form of most momentum-based algorithms can be written into a Hamiltonian descent form:

$$\begin{aligned} \frac{d}{dt} W_t &= -\nabla \mathcal{K}(S) - \Phi_t(\nabla \mathcal{L}(W_t)) \\ \frac{d}{dt} S_t &= \nabla \mathcal{L}(W) - \Psi_t(\nabla \mathcal{K}(S_t)), \end{aligned} \quad (9)$$

where  $H(\mathbf{W}, \mathbf{S})$  is a Hamiltonian (or Lyapunov) function that satisfies

$$\min_S H(\mathbf{W}, \mathbf{S}) = \mathcal{L}(\mathbf{W}), \quad \forall \mathbf{W},$$

so that minimizing  $\mathcal{L}(\mathbf{W})$  reduces to minimizing  $H(\mathbf{W}, \mathbf{S})$ ; and  $\Phi(\cdot), \Psi(\cdot)$  are two monotonic mappings satisfying

$$\|\mathbf{X}\|_{\Phi}^2 := \langle \mathbf{X}, \Phi(\mathbf{X}) \rangle \geq 0, \quad \|\mathbf{X}\|_{\Psi}^2 := \langle \mathbf{X}, \Psi(\mathbf{X}) \rangle \geq 0, \quad \forall \mathbf{X}.$$

With  $\Phi(\mathbf{X}) = \Psi(\mathbf{X}) = 0$ , the system in (9) reduces to the standard Hamiltonian system that keeps  $H(\mathbf{W}_t, \mathbf{S}_t) = \text{const}$  along the trajectory. When adding the descending components with  $\Phi$  and  $\Psi$ , the system then keeps  $H(\mathbf{W}, \mathbf{S})$  monotonically non-decreasing.

It is easy to show that the dynamics monotonically decreases  $\frac{d}{dt} H(W_t, S_t) \leq 0$  since

$$\begin{aligned} \frac{d}{dt} H(W_t, S_t) &= \nabla \mathcal{L}(W)^T \dot{W}_t + \nabla \mathcal{K}(S)^T \dot{S}_t \\ &= \nabla \mathcal{L}(W)^T (-\nabla \mathcal{K}(S) - \Phi_t(\nabla \mathcal{L}(W_t))) + \nabla \mathcal{K}(S)^T (\nabla \mathcal{L}(W) - \Psi_t(\nabla \mathcal{K}(S_t))) \\ &= -\nabla \mathcal{L}(W)^T \Phi_t(\nabla \mathcal{L}(W_t)) - \nabla \mathcal{K}(S)^T \Psi_t(\nabla \mathcal{K}(S_t)) \\ &= -\|\mathbf{X}\|_{\Phi}^2 - \|\mathbf{X}\|_{\Psi}^2, \end{aligned}$$

so that minimizing  $\mathcal{L}(\mathbf{W})$  reduces to minimizing  $H(W, S)$ . However,  $\mathcal{L}(W)$ , which is the true objective, is not necessarily decreasing monotonically.

Because  $H = L + K$ , this means that there are cases when  $L$  increases while  $K$  decreases.

How to change the dynamics to make it *simultaneously* decreases both  $H(W, S)$  and  $\mathcal{L}(W)$ ?

To do so, we modify introduce a modification of the system:

$$\begin{aligned} \frac{d}{dt} W_t &= -\nabla \mathcal{K}(S) \circ \phi(\nabla \mathcal{L}(W) \circ \nabla \mathcal{K}(S)) - \Phi_t(\nabla \mathcal{L}(W_t)) \\ \frac{d}{dt} S_t &= \nabla \mathcal{L}(W) - \Psi_t(\nabla \mathcal{K}(S)), \end{aligned} \quad (10)$$

where  $\circ$  denotes elementwise product. Above update (10) is exactly our C-optimizer's continuous form. Here we introduce a weighting  $\phi(\nabla \mathcal{L}(W) \circ \nabla \mathcal{K}(S))$  on the update direction of  $W_t$  based on the product of  $\nabla \mathcal{L}(W)$  and  $\nabla \mathcal{K}(S)$ .

The following conditions on the choice of function  $\phi$  ensures that the system simultaneously decreases both  $H$  and  $L$  simultaneously.

**Theorem A.1.** *The following inequalities hold under specific conditions on  $x$  and  $\phi(x)$ :*

- If  $x \cdot (1 - \phi(x)) \leq 0$ , then  $\frac{d}{dt} H(W_t, S_t) \leq 0$ .
- If  $x \cdot \phi(x) \geq 0$ , then  $\frac{d}{dt} \mathcal{L}(W_t) \leq 0$ .

**Remark** The function  $\phi(x) = \mathbb{I}(x \geq 0)$  is a simple choice that satisfies both conditions, while being the closest to a constant function. For simplicity of notation, we define the norm  $\|X\|_\phi$  as:

$$\|X\|_\phi^2 = \mathbf{1}^\top (X \circ \phi(X)), \quad \forall X.$$

This notation will be used in subsequent derivations.

**Remark** The first condition also implies the rate of decrease in the loss  $L$  for the masked dynamics (9) is at least as large as for the original dynamics (10) as shown in Theorem A.2

*Proof.* For simplicity, we write  $\mathcal{D} = \nabla \mathcal{L}(W) \circ \nabla \mathcal{K}(S)$ .

Following the dynamics in (10), let us see the derivation of  $H$  w.r.t.  $t$ :

$$\begin{aligned} & \frac{d}{dt} H(W_t, S_t) \\ &= \nabla \mathcal{L}(W)^T \dot{W}_t + \nabla \mathcal{K}(S)^T \dot{S}_t \\ &= \nabla \mathcal{L}(W)^T (-\nabla \mathcal{K}(S) \circ \phi(\mathcal{D}) - \Phi_t(\nabla \mathcal{L}(W_t))) + \nabla \mathcal{K}(S)^T (\nabla \mathcal{L}(W) - \Psi_t(\nabla \mathcal{K}(S_t))) \\ &= \nabla \mathcal{L}(W)^T (\nabla \mathcal{K}(S) \circ (\mathbf{1} - \phi(\mathcal{D}))) - \nabla \mathcal{L}(W)^T \Phi_t(\nabla \mathcal{L}(W_t)) - \nabla \mathcal{K}(S)^T \Psi_t(\nabla \mathcal{K}(S_t)) \\ &= \mathbf{1}^T ((\nabla \mathcal{L}(W) \circ \nabla \mathcal{K}(S)) \circ (\mathbf{1} - \phi(\nabla \mathcal{L}(W) \circ \nabla \mathcal{K}(S)))) - \|\nabla \mathcal{L}(W)\|_\Phi^2 - \|\nabla \mathcal{K}(S)\|_\Psi^2 \\ &= \mathbf{1}^T ([\mathcal{D} \circ (\mathbf{1} - \phi(\mathcal{D}))]) - \|\nabla \mathcal{L}(W)\|_\Phi^2 - \|\nabla \mathcal{K}(S)\|_\Psi^2 \end{aligned} \quad (11)$$

Given the fact that  $\phi$  is an element-wise operator, it is noteworthy that if  $x \cdot (1 - \phi(x)) \leq 0$ , then the first term in (11)  $\mathbf{1}^T ((\nabla \mathcal{L}(W) \circ \nabla \mathcal{K}(S)) \circ (\mathbf{1} - \phi(\nabla \mathcal{L}(W) \circ \nabla \mathcal{K}(S)))) \leq 0$  since we see  $\nabla \mathcal{L}(W) \circ \nabla \mathcal{K}(S)$  as  $x$ .

Next, let us look into the derivative of  $\mathcal{L}(W_t)$  w.r.t.  $t$ :

$$\begin{aligned} \frac{d}{dt} \mathcal{L}(W_t) &= \nabla \mathcal{L}(W)^T (-\nabla \mathcal{K}(S) \circ \phi(\nabla \mathcal{L}(W) \circ \nabla \mathcal{K}(S)) - \Phi_t(\nabla \mathcal{L}(W_t))) \\ &= -\nabla \mathcal{L}(W)^T (\nabla \mathcal{K}(S) \circ \phi(\nabla \mathcal{L}(W) \circ \nabla \mathcal{K}(S))) - \nabla \mathcal{L}(W)^T \Phi_t(\nabla \mathcal{L}(W_t)) \\ &= -\mathbf{1}^T (\nabla \mathcal{L}(W) \circ \nabla \mathcal{K}(S) \circ \phi(\nabla \mathcal{L}(W) \circ \nabla \mathcal{K}(S))) - \nabla \mathcal{L}(W)^T \Phi_t(\nabla \mathcal{L}(W_t)). \end{aligned} \quad (12)$$

It is clear that if the first term in (12), namely

$$(\nabla \mathcal{L}(W) \circ \nabla \mathcal{K}(S) \circ \phi(\nabla \mathcal{L}(W) \circ \nabla \mathcal{K}(S))) \geq 0,$$

then  $\frac{d}{dt} \mathcal{L}(W_t) \leq 0$ . This condition is satisfied when  $x \cdot \phi(x) \geq 0$ .  $\square$

**Theorem A.2.** Consider the two dynamical systems defined by (9) and (10). If the conditions in Theorem A.1 hold, then the rate of decrease in the loss  $L$  for the masked dynamics (9) is at least as large as for the original dynamics (10). Specifically, we have:

$$\nabla \mathcal{L}(W_t)^\top U_t \leq \nabla \mathcal{L}(W_t)^\top V_t, \quad (13)$$

where

$$\begin{aligned} U_t &= -\nabla \mathcal{K}(S_t) \circ \phi(\nabla \mathcal{L}(W_t) \circ \nabla \mathcal{K}(S_t)) - \Phi_t(\nabla \mathcal{L}(W_t)), \\ V_t &= -\nabla \mathcal{K}(S_t) - \Phi_t(\nabla \mathcal{L}(W_t)). \end{aligned}$$

**Remark** The momentum methods monotonically decreases  $H(W, S)$ , but the loss  $L$  can increase temporarily (although eventually go down as  $L$  is a part of  $H$ ). So C optimizer suppresses any temporarily increase of  $L$ , without hurting the monotonically increase of  $H$ .

**Theorem A.3.** Let  $(W_t, S_t)$  and  $(\bar{W}_t, \bar{S}_t)$  denote the solutions to the initial value problems (IVPs) associated with the dynamical systems (10) and (9), respectively, with shared initial conditions  $W_0 = \bar{W}_0$  and  $S_0 = \bar{S}_0$ , and  $\Phi = 0$ .

Then, for all  $t \geq 0$ , the following inequality holds:

$$\mathcal{L}(W_t) \leq \mathcal{L}(\bar{W}_t),$$

where  $\mathcal{L}(\cdot)$  represents the loss (or energy) functional associated with the system. This inequality implies that the solution trajectory  $(\bar{W}_t, \bar{S}_t)$  maintains a loss value that does not exceed that of the trajectory  $(W_t, S_t)$  at any point in time.

*Proof.* The proof proceeds by contradiction. Assume that there exists some  $\tau > 0$  such that

$$\mathcal{L}(W_\tau) > \mathcal{L}(\bar{W}_\tau).$$

Since the initial conditions satisfy  $\mathcal{L}(W_0) = \mathcal{L}(\bar{W}_0)$ , there must exist a time  $\tau_0 \in (0, \tau)$  such that the two trajectories intersect at this point, i.e.,

$$\mathcal{L}(W_{\tau_0}) = \mathcal{L}(\bar{W}_{\tau_0}),$$

and  $\exists \delta > 0$ , such that

$$\forall \epsilon \in (0, \delta), \quad \mathcal{L}(\bar{W}_{\tau_0+\epsilon}) < \mathcal{L}(W_{\tau_0+\epsilon}).$$

Consider the changes in the loss functional around  $\tau_0 + \epsilon$ :

$$\mathcal{L}(\bar{W}_{\tau_0+\epsilon}) - \mathcal{L}(\bar{W}_{\tau_0}) < \mathcal{L}(W_{\tau_0+\epsilon}) - \mathcal{L}(W_{\tau_0}).$$

Dividing through by  $\epsilon$  and taking the limit as  $\epsilon \rightarrow 0$ , we have:

$$\lim_{\epsilon \rightarrow 0} \frac{\mathcal{L}(\bar{W}_{\tau_0+\epsilon}) - \mathcal{L}(\bar{W}_{\tau_0})}{\epsilon} \leq \lim_{\epsilon \rightarrow 0} \frac{\mathcal{L}(W_{\tau_0+\epsilon}) - \mathcal{L}(W_{\tau_0})}{\epsilon}.$$

By the definition of the derivative of  $\mathcal{L}$ , this becomes:

$$\frac{d}{dt} \mathcal{L}(\bar{W}_{\tau_0}) \leq \frac{d}{dt} \mathcal{L}(W_{\tau_0}),$$

If  $\frac{d}{dt} \mathcal{L}(\bar{W}_{\tau_0}) = \frac{d}{dt} \mathcal{L}(W_{\tau_0})$ , then by Theorem A.2, we have

$$\mathbf{1}^T ([\mathcal{D} \circ (\mathbf{1} - \phi(\mathcal{D}))]) = 0,$$

Note that  $x\phi(x) \geq \max(x, 0)$ , here we pick  $\phi(x) = (1 + \epsilon)\mathbb{I}(x \geq 0)$  with  $\epsilon > 0$ .

Thus, it follows  $\mathcal{D} = 0$ , and hence  $\frac{d}{dt} \mathcal{L}(\bar{\mathbf{w}}_{\tau_0}) = \frac{d}{dt} \mathcal{L}(\mathbf{w}_{\tau_0}) = 0$ , which means  $\mathbf{w}_{\tau_0} = \bar{\mathbf{w}}_{\tau_0}$  is a stationary point of  $\mathcal{L}$ .

We have which translates to:

$$\nabla \mathcal{L}(\bar{W}_{\tau_0})^\top V_{\tau_0} < \nabla \mathcal{L}(W_{\tau_0})^\top U_{\tau_0}.$$

From Theorem A.2, we know that for the corresponding systems, the velocity vectors satisfy:

$$\nabla \mathcal{L}(W_t)^\top V_t \leq \nabla \mathcal{L}(W_t)^\top U_t.$$

However, this contradicts the assumption that  $\nabla \mathcal{L}(\bar{W}_{\tau_0})^\top V_{\tau_0} < \nabla \mathcal{L}(W_{\tau_0})^\top U_{\tau_0}$ .

Thus, the assumption that  $\mathcal{L}(W_\tau) > \mathcal{L}(\bar{W}_\tau)$  must be false, and we conclude:

$$\mathcal{L}(W_t) \leq \mathcal{L}(\bar{W}_t), \quad \forall t \geq 0.$$

□

**Corollary A.4.** Assume  $\|\cdot\|_{\Psi}^2$  is positive definite and  $\Psi(0) = 0$ , and  $H(\mathbf{w}, \mathbf{s}) = \mathcal{L}(\mathbf{w}) + \mathcal{K}(\mathbf{s})$  is differentiable, then the original system (9) converges to a stationary point of  $H(W, S)$ , and (10) also converges to a stationary point of  $H(W, S)$ .

*Proof.* First, we use LaSalle's invariance principle to find the conditions that the accumulation points (positive limit points) satisfy:

$$\text{System (9): } \|\nabla\mathcal{L}(W)\|_{\Phi}^2 = \|\nabla\mathcal{K}(S)\|_{\Psi}^2 = 0,$$

$$\text{System (10): } \|\nabla\mathcal{L}(W)\|_{\Phi}^2 = \|\nabla\mathcal{K}(S)\|_{\Psi}^2 = 0, \mathbf{1}^T(\mathcal{D} \circ (\mathbf{1} - \phi(\mathcal{D}))) = 0.$$

By the assumption that  $\|\cdot\|_{\Psi}^2$  is positive definite and  $\Psi(0) = 0$ , we have  $\nabla\mathcal{K}(S) = 0$ .

For positive limit points of systems (10) and (9), if  $\nabla\mathcal{L}(W) \neq 0$ , then the point  $(W, S)$  is not a positive limit point since

$$\dot{S} = \nabla\mathcal{L}(W) - \Psi(\nabla\mathcal{K}(S)) = \nabla\mathcal{L}(W) \neq 0.$$

Thus,  $\nabla\mathcal{L}(W) = 0$ . Together with  $\nabla\mathcal{K}(S) = 0$ , we conclude that  $(W, S)$  is a stationary point of  $H(W, S)$ .  $\square$

**Theorem A.5.** Assuming  $\mathcal{L}(W)$  is convex, for the following update schemes:

$$\text{Cautious Momentum} \begin{cases} W_{t+1} = W_t - \varepsilon M_{t+1} \cdot \mathbb{1}_{\nabla\mathcal{L}(W_t)^\top M_{t+1} \geq 0}, \\ M_{t+1} = M_t - \varepsilon \nabla\mathcal{L}(W_t), \end{cases} \quad \text{Momentum} \begin{cases} W_{t+1} = W_t - \varepsilon M_{t+1}, \\ M_{t+1} = M_t - \varepsilon \nabla\mathcal{L}(W_t), \end{cases}$$

we have that Cautious Momentum is at least as fast as Momentum.

*Proof.* For the Momentum update, we have

$$\begin{aligned} \mathcal{L}(W_{t+1}) - \mathcal{L}(W_t) &\geq \nabla\mathcal{L}(W_t)^\top (W_{t+1} - W_t) \quad //\text{By convexity of } \mathcal{L}, \\ &= -\varepsilon \nabla\mathcal{L}(W_t)^\top M_{t+1}. \end{aligned}$$

If  $\nabla\mathcal{L}(W_t)^\top M_{t+1} < 0$ , then  $\mathcal{L}(W_{t+1}) - \mathcal{L}(W_t) \geq 0$ , which means  $\mathcal{L}$  increases at this step.

For the Cautious Momentum update, we have

$$\begin{aligned} \mathcal{L}(W_{t+1}) - \mathcal{L}(W_t) &\geq \nabla\mathcal{L}(W_t)^\top (W_{t+1} - W_t) \quad //\text{By convexity of } \mathcal{L}, \\ &= -\varepsilon \nabla\mathcal{L}(W_t)^\top M_{t+1} \cdot \mathbb{1}_{\nabla\mathcal{L}(W_t)^\top M_{t+1} \geq 0}. \end{aligned}$$

If  $\nabla\mathcal{L}(W_t)^\top M_{t+1} < 0$ , then  $\mathbb{1}_{\nabla\mathcal{L}(W_t)^\top M_{t+1} \geq 0} = 0$ , and thus  $W_{t+1} = W_t$ .

If  $\nabla\mathcal{L}(W_t)^\top M_{t+1} \geq 0$ , then  $\mathbb{1}_{\nabla\mathcal{L}(W_t)^\top M_{t+1} \geq 0} = 1$ , and Cautious Momentum follows the same update scheme as Momentum.

Hence, Cautious Momentum is at least as fast as Momentum.  $\square$

**Theorem A.6.** Assuming  $\mathcal{L}(W)$  is  $L$ -smooth, for the following update schemes:

$$\text{Cautious Momentum} \begin{cases} W_{t+1} = W_t - \varepsilon M_{t+1} \cdot \mathbb{1}_{\nabla\mathcal{L}(W_t)^\top M_{t+1} \geq -\frac{L\varepsilon}{2} \|M_{t+1}\|^2}, \\ M_{t+1} = M_t - \varepsilon \nabla\mathcal{L}(W_t), \end{cases} \quad \text{Momentum} \begin{cases} W_{t+1} = W_t - \varepsilon M_{t+1}, \\ M_{t+1} = M_t - \varepsilon \nabla\mathcal{L}(W_t), \end{cases}$$

we have that Cautious Momentum is at least as good as Momentum with any step size  $\varepsilon > 0$ .

*Proof.* For Momentum update scheme,

$$\begin{aligned} \mathcal{L}(W_t) - \mathcal{L}(W_{t+1}) &\leq -\nabla\mathcal{L}(W_t)^\top (W_{t+1} - W_t) + \frac{L}{2} \|W_{t+1} - W_t\|^2 \quad //\text{By } L\text{-smoothness of } \mathcal{L} \\ &= \varepsilon \nabla\mathcal{L}(W_t)^\top M_{t+1} + \frac{\varepsilon^2 L}{2} \|M_{t+1}\|^2. \end{aligned}$$

If  $\nabla\mathcal{L}(W_t)^\top M_{t+1} + \frac{\varepsilon L}{2} \|M_{t+1}\|^2 < 0$ , then at this step,  $\mathcal{L}$  is actually increasing.

While for Cautious Momentum update,

$$\mathcal{L}(W_t) - \mathcal{L}(W_{t+1}) \leq \varepsilon \left( \nabla\mathcal{L}(W_t)^\top M_{t+1} + \frac{\varepsilon^2 L}{2} \|M_{t+1}\|^2 \right) \cdot \mathbb{1}_{\nabla\mathcal{L}(W_t)^\top M_{t+1} \geq -\frac{L\varepsilon}{2} \|M_{t+1}\|^2}$$

If  $\nabla\mathcal{L}(W_t)^\top M_{t+1} + \frac{\varepsilon L}{2} \|M_{t+1}\|^2 < 0$ , then at this step,  $\mathbb{1}_{\nabla\mathcal{L}(W_t)^\top M_{t+1} \geq -\frac{L\varepsilon}{2} \|M_{t+1}\|^2} = 0$ , thus,  $W_{t+1} = W_t$ .

If  $\nabla\mathcal{L}(W_t)^\top M_{t+1} + \frac{\varepsilon L}{2} \|M_{t+1}\|^2 > 0$ , then  $\mathbb{1}_{\nabla\mathcal{L}(W_t)^\top M_{t+1} \geq -\frac{L\varepsilon}{2} \|M_{t+1}\|^2} = 1$ . Hence, Cautious Momentum follows the same update scheme as Momentum.  $\square$

## A.2. Examples

We instantiate the result on Adam, SignGD, and Lion below.

### A.2.1. ADAM

$$\begin{aligned} \frac{dW}{dt} &= -\frac{M_t}{\sqrt{V_t} + \varepsilon} \\ \frac{d}{dt}M_t &= \beta_1 \cdot (\nabla\mathcal{L}(W_t) - M_t) \\ \frac{d}{dt}V_t &= \beta_2 \cdot (\nabla\mathcal{L}(W_t)^{\odot 2} - V_t) \end{aligned}$$

with

$$H(W, M, V) = \mathcal{L}(W) + \frac{1}{2\beta_1} \left\langle \frac{M}{\sqrt{V} + \varepsilon}, M \right\rangle \quad (14)$$

$$\begin{aligned} \frac{dH(W, M, V)}{dt} &= \left\langle \nabla\mathcal{L}(W_t), \frac{dW}{dt} \right\rangle + \frac{1}{2\beta_1} \cdot \left( \left\langle \frac{2M_t}{\sqrt{V_t} + \varepsilon}, \frac{dM}{dt} \right\rangle + \left\langle \frac{-M_t^{\odot 2} \odot \frac{1}{2\sqrt{V_t}}}{(\sqrt{V_t} + \varepsilon)^{\odot 2}}, \frac{dV}{dt} \right\rangle \right) \\ &= -\left\langle \frac{M_t}{\sqrt{V_t} + \varepsilon}, M_t \right\rangle - \frac{\beta_2}{4\beta_1} \left\langle \frac{M_t^{\odot 2}}{V_t^{3/2} + \varepsilon}, \nabla\mathcal{L}(W_t)^{\odot 2} \right\rangle + \left\langle \frac{M_t^{\odot 2}}{V_t^{3/2} + \varepsilon}, V_t \right\rangle \\ &= -\frac{\beta_2}{4\beta_1} \left\langle \frac{M_t^{\odot 2}}{V_t^{3/2} + \varepsilon}, \nabla\mathcal{L}(W_t)^{\odot 2} \right\rangle - (1 - \frac{\beta_2}{4\beta_1}) \left\langle \frac{M_t}{\sqrt{V_t} + \varepsilon}, M_t \right\rangle \end{aligned}$$

We want  $\frac{dH(W, M, V)}{dt} \leq 0$  always, hence  $1 - \frac{\beta_2}{4\beta_1} \geq 0$ , thus  $\beta_1 \geq \frac{\beta_2}{4}$

### A.2.2. CAUTIOUS ADAM

$$\begin{aligned} \frac{dW}{dt} &= -\frac{\mathbb{1}(\text{sign}(\nabla\mathcal{L}(W_t)) = \text{sign}(M_t)) \circ M_t}{\sqrt{V_t} + \varepsilon} \\ \frac{d}{dt}M_t &= \beta_1 \cdot (\nabla\mathcal{L}(W_t) - M_t) \\ \frac{d}{dt}V_t &= \beta_2 \cdot (\nabla\mathcal{L}(W_t)^{\odot 2} - V_t). \end{aligned}$$

It is easy to show that the loss function  $\mathcal{L}(W_t)$  itself is a Hamiltonian (Lyapunov) since

$$\frac{d}{dt}\mathcal{L}(W_t) = -\nabla\mathcal{L}(W_t)^\top \dot{W}_t = -\nabla\mathcal{L}(W_t)^\top \left( \frac{\mathbb{1}(\text{sign}(\nabla\mathcal{L}(W_t)) = \text{sign}(M_t)) \circ M_t}{\sqrt{V_t} + \varepsilon} \right) \leq 0.$$

### A.2.3. SIGNGD

Recall the update scheme of sign momentum (Bernstein et al., 2018):

$$\begin{aligned}\dot{W} &= -\text{sign}(M) \\ \dot{M} &= \nabla\mathcal{L}(W) - M.\end{aligned}$$

We can verify that the following is a Hamiltonian for above dynamic system:

$$H(W, M) = \mathcal{L}(W) + \|M\|_1,$$

it's simple to verify

$$\dot{H} = -\nabla\mathcal{L}(W)^\top \text{sign}(M) + \text{sign}(M)^\top \nabla\mathcal{L}(W) - \|M\|_1 = -\|M\|_1.$$

### A.2.4. CAUTIOUS SIGNSGD

Recall the update scheme of cautious sign momentum:

$$\begin{aligned}\dot{W} &= -\text{sign}(M) \odot \mathbb{1}_{\text{sign}(\nabla\mathcal{L}(W))=\text{sign}(M)} \\ \dot{M} &= \nabla\mathcal{L}(W) - M.\end{aligned}$$

We can verify that the loss function itself is Hamiltonian (a Lyapunov):

$$\frac{d}{dt}\mathcal{L}(W) = \nabla\mathcal{L}(W)^\top \dot{W}_t = -\nabla\mathcal{L}(W)^\top (\text{sign}(M) \odot \mathbb{1}_{\text{sign}(\nabla\mathcal{L}(W))=\text{sign}(M)}) = -\|\nabla\mathcal{L}(W) \odot \mathbb{1}_{\text{sign}(\nabla\mathcal{L}(W))=\text{sign}(M)}\|_1.$$

### A.2.5. LION

Recall the update of Lion (Chen et al., 2023a):

$$\begin{aligned}\dot{M}_t &= \alpha\nabla\mathcal{L}(W_t) - \gamma M_t \\ \dot{W}_t &= -\text{sign}(\tilde{M}_t),\end{aligned}$$

with  $\gamma, \alpha > 0$ , and  $\tilde{M} = M - \varepsilon(\alpha\nabla\mathcal{L}(W) + \gamma M)$ .

Following the derivation in (Chen et al., 2023a), we have the following Hamiltonian (Lyapunov) function:

$$H(W, M) = \alpha\mathcal{L}(W) + (1 - \varepsilon\gamma) \|M\|_1.$$

Since

$$\begin{aligned}\dot{H}(W, M) &= \alpha\nabla\mathcal{L}(W)^\top \dot{W} + (1 - \varepsilon\gamma)\text{sign}(M)^\top \dot{M} \\ &= -\alpha\nabla\mathcal{L}(W)^\top (\text{sign}(\tilde{M})) + (1 - \varepsilon\gamma)\text{sign}(M)^\top (\alpha\nabla\mathcal{L}(W) - \gamma M) \\ &= -(1 - \varepsilon\gamma)(\text{sign}(\tilde{M}) - \text{sign}(M))^\top (M - \tilde{M}) - \gamma \|\tilde{M}\|_1,\end{aligned}$$

where  $1 - \varepsilon\gamma \geq 0$ .

### A.2.6. CAUTIOUS LION

$$\dot{M} = \alpha\nabla\mathcal{L}(W) - \gamma M \tag{15}$$

$$\dot{W} = -\text{sign}(\tilde{M}) \odot \mathbb{1}_{\text{sign}(\nabla\mathcal{L}(W))=\text{sign}(\tilde{M})}, \tag{16}$$

where  $\tilde{M} = M - \varepsilon(\alpha\nabla\mathcal{L}(W) + \gamma M)$ .

The loss function  $f(\cdot)$  itself is a Hamiltonian since

$$\dot{\mathcal{L}}(W) = \nabla\mathcal{L}(W)^\top \dot{W} = \nabla\mathcal{L}(W)^\top (\text{sign}(\tilde{M}) \odot \mathbb{1}_{\text{sign}(\nabla\mathcal{L}(W))=\text{sign}(\tilde{M})}) = -\|\nabla\mathcal{L}(W) \odot \mathbb{1}_{\text{sign}(\nabla\mathcal{L}(W))=\text{sign}(\tilde{M})}\|_1.$$

### A.3. From Continuous Time to Discrete time

This subsection should be after the continuous analysis of Hamiltonian, we can show the decreasing of the loss of c-optimizer is simply larger or equal to baseline optimizer at each iteration from a discrete time perspective.

First, by discretizing dynamical system (9), we have

$$\begin{aligned} W_{t+1} &:= W_t + \varepsilon U_t = W_t - \varepsilon (\nabla \mathcal{K}(S_t) \circ \phi(\nabla \mathcal{L}(W_t) \circ \nabla K(S_t)) + \Phi_t(\nabla \mathcal{L}(W_t))) \\ S_{t+1} &:= S_t + \varepsilon (\nabla \mathcal{L}(W_t) - \Psi_t(\nabla \mathcal{K}(S_t))). \end{aligned} \quad (17)$$

By discretizing dynamical system (10), we have

$$\begin{aligned} W_{t+1} &:= W_t + \varepsilon V_t = W_t - \varepsilon (\nabla \mathcal{K}(S_t) + \Phi_t(\nabla \mathcal{L}(W_t))) \\ S_{t+1} &:= S_t + \varepsilon (\nabla \mathcal{L}(W_t) - \Psi_t(\nabla \mathcal{K}(S_t))) \end{aligned} \quad (18)$$

**Theorem A.7.** [Larger Loss Decreasing] Assume loss function  $\mathcal{L}(\cdot)$  is differentiable and  $L$ -smooth, and element-wise operator  $\phi$  satisfies  $x \cdot (1 - \phi(x)) \leq 0$  and  $x \cdot \phi(x) \geq 0$ .

For the discretized update,

$$\begin{aligned} W_{t+1} &= W_t + \varepsilon U_t \\ \bar{W}_{t+1} &= W_t + \varepsilon V_t, \end{aligned} \quad (19)$$

we have

$$\mathcal{L}(W_t + \varepsilon U_t) \leq \mathcal{L}(W_t + \varepsilon V_t), \quad \text{i.e. } \mathcal{L}(W_{t+1}) \leq \mathcal{L}(\bar{W}_{t+1}),$$

where  $\varepsilon \leq \frac{2\|\nabla \mathcal{L}(W_t) \circ \nabla K(S_t)\|_{\Phi}^2 + 2\|\nabla \mathcal{L}(W_t)\|_{\Phi}^2}{\|\mathcal{R}_t\|(2L \cdot \|V_t\| + \|\mathcal{R}_t\|)}$  and  $\mathcal{R}_t = U_t - V_t$ .

*Proof.* First, we calculate the difference between  $W_{t+1}$  and  $\bar{W}_{t+1}$ , then we use  $L$ -smooth condition to bound the difference between  $\mathcal{L}(W_{t+1})$  and  $\mathcal{L}(\bar{W}_{t+1})$ .

$$\begin{aligned} W_{t+1} - \bar{W}_{t+1} &= \varepsilon(U_t - V_t) \\ &= \varepsilon(\nabla \mathcal{K}(S_t) + \Phi_t(\nabla \mathcal{L}(W_t)) - \nabla \mathcal{K}(S_t) \circ \phi(\nabla \mathcal{L}(W_t) \circ \nabla K(S_t)) - \Phi_t(\nabla \mathcal{L}(W_t))) \\ &= \varepsilon \nabla \mathcal{K}(S_t) \circ (\mathbf{1} - \phi(\nabla \mathcal{L}(W_t) \circ \nabla K(S_t))) \\ &= \varepsilon \mathcal{R}_t. \end{aligned}$$

Let us use  $L$ -smooth condition to bound the  $\mathcal{L}$  difference

$$\begin{aligned} &\mathcal{L}(W_{t+1}) - \mathcal{L}(\bar{W}_{t+1}) \\ &\leq \varepsilon \cdot \nabla \mathcal{L}(W_{t+1})^\top (\nabla \mathcal{K}(S_t) \circ (\mathbf{1} - \phi(\nabla \mathcal{L}(W_t) \circ \nabla K(S_t)))) + \frac{1}{2} \varepsilon^2 \|\mathcal{R}_t\|^2 \\ &= \varepsilon \cdot (\nabla \mathcal{L}(W_t) + \nabla \mathcal{L}(W_{t+1}) - \nabla \mathcal{L}(W_{t+1}))^\top (\nabla \mathcal{K}(S_t) \circ (\mathbf{1} - \phi(\nabla \mathcal{L}(W_t) \circ \nabla K(S_t)))) + \frac{1}{2} \varepsilon^2 \|\mathcal{R}_t\|^2 \\ &= \varepsilon \cdot \nabla \mathcal{L}(W_t)^\top (\nabla \mathcal{K}(S_t) \circ (\mathbf{1} - \phi(\nabla \mathcal{L}(W_t) \circ \nabla K(S_t)))) \\ &\quad + \varepsilon \cdot (\nabla \mathcal{L}(W_{t+1}) - \nabla \mathcal{L}(W_{t+1}))^\top (\nabla \mathcal{K}(S_t) \circ (\mathbf{1} - \phi(\nabla \mathcal{L}(W_t) \circ \nabla K(S_t)))) + \frac{1}{2} \varepsilon^2 \|\mathcal{R}_t\|^2 \\ &= \varepsilon \cdot \nabla \mathcal{L}(W_t)^\top (\nabla \mathcal{K}(S_t) \circ (\mathbf{1} - \phi(\nabla \mathcal{L}(W_t) \circ \nabla K(S_t)))) \\ &\quad + \varepsilon \cdot L \cdot \|W_{t+1} - W_t\| \cdot \|\nabla \mathcal{K}(S_t) \circ (\mathbf{1} - \phi(\nabla \mathcal{L}(W_t) \circ \nabla K(S_t)))\| + \frac{1}{2} \varepsilon^2 \|\mathcal{R}_t\|^2 \\ &= \varepsilon \cdot \nabla \mathcal{L}(W_t)^\top (\nabla \mathcal{K}(S_t) \circ (\mathbf{1} - \phi(\nabla \mathcal{L}(W_t) \circ \nabla K(S_t)))) \\ &\quad + \varepsilon^2 \cdot L \cdot \|\nabla \mathcal{K}(S_t) + \Phi_t(\nabla \mathcal{L}(W_t))\| \cdot \|\nabla \mathcal{K}(S_t) \circ (\mathbf{1} - \phi(\nabla \mathcal{L}(W_t) \circ \nabla K(S_t)))\| + \frac{1}{2} \varepsilon^2 \|\mathcal{R}_t\|^2 \\ &= \varepsilon \cdot \left( \|\nabla \mathcal{L}(W_t) \circ \nabla K(S_t)\|_{\Phi}^2 + \|\nabla \mathcal{L}(W_t)\|_{\Phi}^2 \right) + \varepsilon^2 \cdot L \cdot \|\mathcal{R}_t\| \cdot \|V_t\| + \frac{1}{2} \varepsilon^2 \|\mathcal{R}_t\|^2 \\ &\leq 0. \quad // \text{By the choice of } \varepsilon. \end{aligned}$$

□



**Theorem A.8** (Convergence Rate for C-Optimizers). *Assume  $\mathcal{L}(W)$  is  $L$ -smooth and differentiable, and the element-wise operator  $\phi$  satisfies  $x \cdot (1 - \phi(x)) \leq 0$  and  $x \cdot \phi(x) \geq 0$  as shown in Theorem A.1. With  $(W_t, S_t)$  following the update in (17):*

$$\begin{aligned} W_{t+1} &:= W_t + \varepsilon U_t = W_t - \varepsilon (\nabla \mathcal{K}(S_t) \circ \phi(\nabla \mathcal{L}(W_t) \circ \nabla \mathcal{K}(S_t)) + \Phi_t(\nabla \mathcal{L}(W_t))), \\ S_{t+1} &:= S_t + \varepsilon (\nabla \mathcal{L}(W_t) - \Psi_t(\nabla \mathcal{K}(S_t))). \end{aligned}$$

Assume  $\varepsilon > 0$ , we have:

$$\frac{1}{T} \sum_{t=1}^T \left( \|\nabla \mathcal{L}(W_t) \circ \nabla \mathcal{K}(S_t)\|_{\phi}^2 + \|\nabla \mathcal{L}(W_t)\|_{\Phi}^2 \right) \leq \frac{\mathcal{L}(W_0) - \mathcal{L}(W^*)}{T\varepsilon} + \frac{L\varepsilon}{2T} B_T,$$

where  $B_T = \sum_{t=1}^T \|U_t\|^2$ .

*Proof.* Using the  $L$ -smoothness of  $\mathcal{L}(W)$ , we expand  $\mathcal{L}(W_{t+1}) - \mathcal{L}(W_t)$ :

$$\mathcal{L}(W_{t+1}) - \mathcal{L}(W_t) \leq \nabla \mathcal{L}(W_t)^\top (W_{t+1} - W_t) + \frac{L}{2} \|W_{t+1} - W_t\|^2.$$

Substitute  $W_{t+1} - W_t = \varepsilon U_t$ , where:

$$U_t = -(\nabla \mathcal{K}(S_t) \circ \phi(\nabla \mathcal{L}(W_t) \circ \nabla \mathcal{K}(S_t)) + \Phi_t(\nabla \mathcal{L}(W_t))),$$

to get:

$$\begin{aligned} \mathcal{L}(W_{t+1}) - \mathcal{L}(W_t) &\leq \varepsilon \cdot \nabla \mathcal{L}(W_t)^\top (\nabla \mathcal{K}(S_t) \circ \phi(\nabla \mathcal{L}(W_t) \circ \nabla \mathcal{K}(S_t)) + \Phi_t(\nabla \mathcal{L}(W_t))) \\ &\quad + \frac{L\varepsilon^2}{2} \|\nabla \mathcal{K}(S_t) \circ \phi(\nabla \mathcal{L}(W_t) \circ \nabla \mathcal{K}(S_t)) + \Phi_t(\nabla \mathcal{L}(W_t))\|^2. \end{aligned}$$

Simplify using the definition of  $\|\cdot\|_{\phi}$  and  $\|\cdot\|_{\Phi}$ :

$$-\nabla \mathcal{L}(W_t)^\top (\nabla \mathcal{K}(S_t) \circ \phi(\nabla \mathcal{L}(W_t) \circ \nabla \mathcal{K}(S_t)) + \Phi_t(\nabla \mathcal{L}(W_t))) = -\|\nabla \mathcal{L}(W_t) \circ \nabla \mathcal{K}(S_t)\|_{\phi}^2 - \|\nabla \mathcal{L}(W_t)\|_{\Phi}^2,$$

which gives:

$$\mathcal{L}(W_{t+1}) - \mathcal{L}(W_t) \leq -\varepsilon \left( \|\nabla \mathcal{L}(W_t) \circ \nabla \mathcal{K}(S_t)\|_{\phi}^2 + \|\nabla \mathcal{L}(W_t)\|_{\Phi}^2 \right) + \frac{L\varepsilon^2}{2} \|U_t\|^2.$$

Summing over  $t = 1, \dots, T$ , we obtain a telescoping sum:

$$\mathcal{L}(W_{T+1}) - \mathcal{L}(W_1) \leq -\varepsilon \sum_{t=1}^T \left( \|\nabla \mathcal{L}(W_t) \circ \nabla \mathcal{K}(S_t)\|_{\phi}^2 + \|\nabla \mathcal{L}(W_t)\|_{\Phi}^2 \right) + \frac{L\varepsilon^2}{2} \sum_{t=1}^T \|U_t\|^2.$$

Rearranging, dividing by  $T\varepsilon$ , and noting  $\mathcal{L}(W_{T+1}) \geq \mathcal{L}(W^*)$ , we get:

$$\frac{1}{T} \sum_{t=1}^T \left( \|\nabla \mathcal{L}(W_t) \circ \nabla \mathcal{K}(S_t)\|_{\phi}^2 + \|\nabla \mathcal{L}(W_t)\|_{\Phi}^2 \right) \leq \frac{\mathcal{L}(W_1) - \mathcal{L}(W^*)}{T\varepsilon} + \frac{L\varepsilon}{2T} B_T,$$

where  $B_T = \sum_{t=1}^T \|U_t\|^2$ . This concludes the proof.  $\square$

#### A.4. Pseudo Code

## B. Experiment Details

All experiments are run on a 4×80G A100 DGX box.

**Algorithm 3** C-Lion Optimizer

**Require:** learning rate  $\epsilon$ , momentum coefficient  $\beta_1, \beta_2 \in [0, 1)$ , weight decay factor  $\gamma$

```

1: Initialize parameter vector  $w_t$ 
2: Initialize  $t = 0, m_0 = \mathbf{0}$ 
3: while  $w_t$  not converged do
4:    $t \leftarrow t + 1$ 
5:    $g_t \leftarrow \nabla_w \mathcal{L}_t(w_{t-1})$                                 {Get gradients at timestep  $t$ }
6:    $u_t \leftarrow \text{sign}(\beta_1 m_{t-1} + (1 - \beta_1) \cdot g_t)$           {get the signed update}
7:    $m_t \leftarrow \beta_2 m_{t-1} + (1 - \beta_2) \cdot g_t$               {update momentum}
8:    $\phi_t \leftarrow \mathbb{I}(u_t \circ g_t \geq 0)$                           // Compute alignment mask
9:    $\bar{\epsilon}_t = \epsilon_t \frac{d}{\|\phi_t\|_0 + 1}$                        // Scale lr,  $d$  is dimension of  $\phi_t$ 
10:   $w_t \leftarrow w_{t-1} - \bar{\epsilon}_t \phi_t \circ u_t$ 
11:   $w_t \leftarrow w_t - \epsilon \gamma w_t$                                {Weight decay}
12: end while

```

# Params	$\beta_1$	$\beta_2$	Learning rate (AdamW)	Learning rate (Lion)	weight decay	Batch Size
60 M	0.9	0.99	0.001	0.0001	0.0	512
100 M	0.9	0.99	0.001	0.0001	0.0	512
350 M	0.9	0.99	0.001	0.0001	0.0	1024
1B	0.9	0.95	0.001	0.0001	0.1	2048

Table 4: Hyperparameters for LLM experiments. For 60M, 100M and 350M, we use  $\beta_1 = 0.9, \beta_2 = 0.99$  and weight decay 0.0 on AdamW; For 1B model, we find  $\beta_1 = 0.9, \beta_2 = 0.95$  and weight decay 0.1 yeild the best results. Sequence length of all models are 256.

# Params	$\beta_1$	$\beta_2$	Learning rate	weight decay	Batch Size
110 M	0.9	0.999	$1.5 \times 10^{-4}$	0.05	4096

Table 5: Hyperparameters for MAE experiment

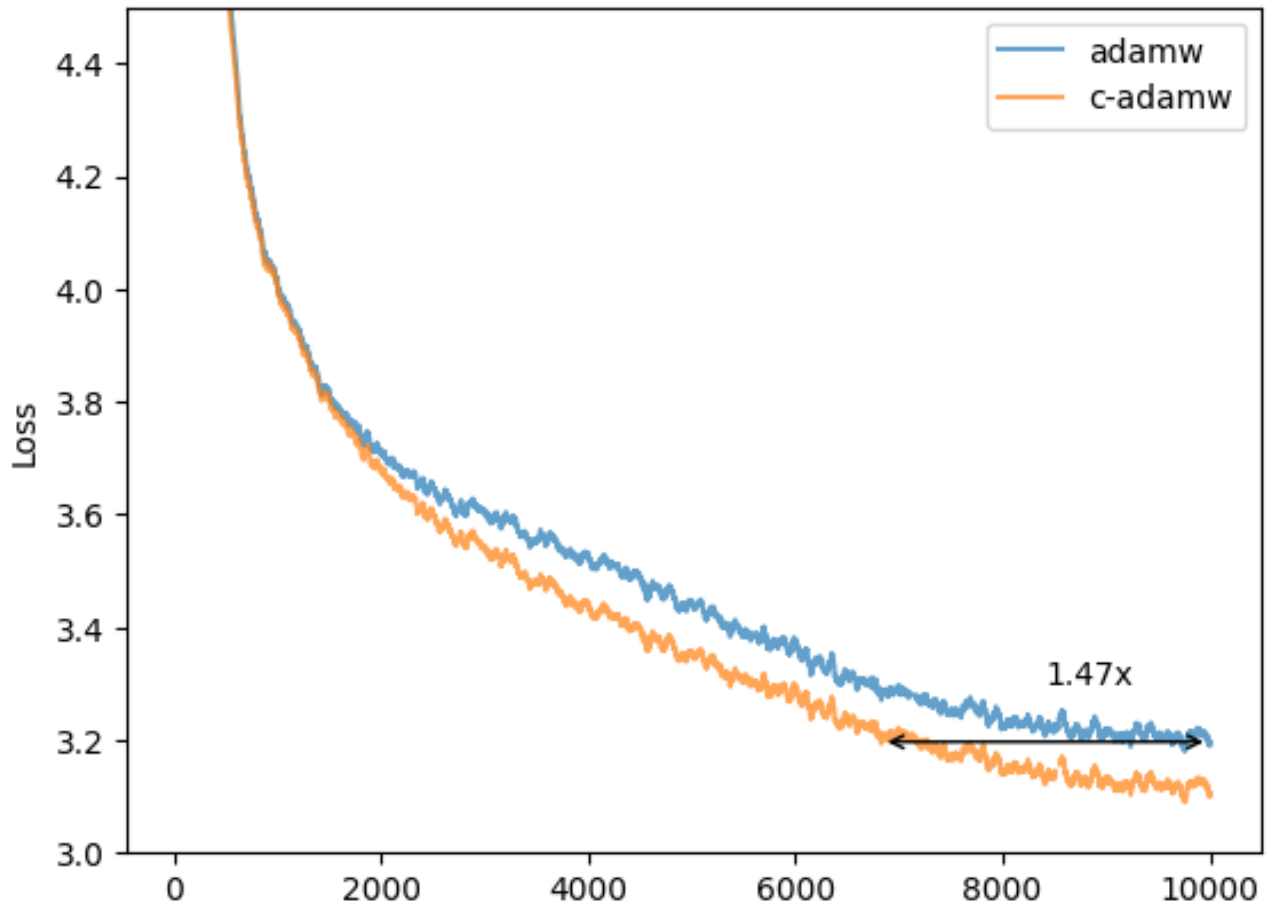


Figure 5: 1.47x speed up on AdamW

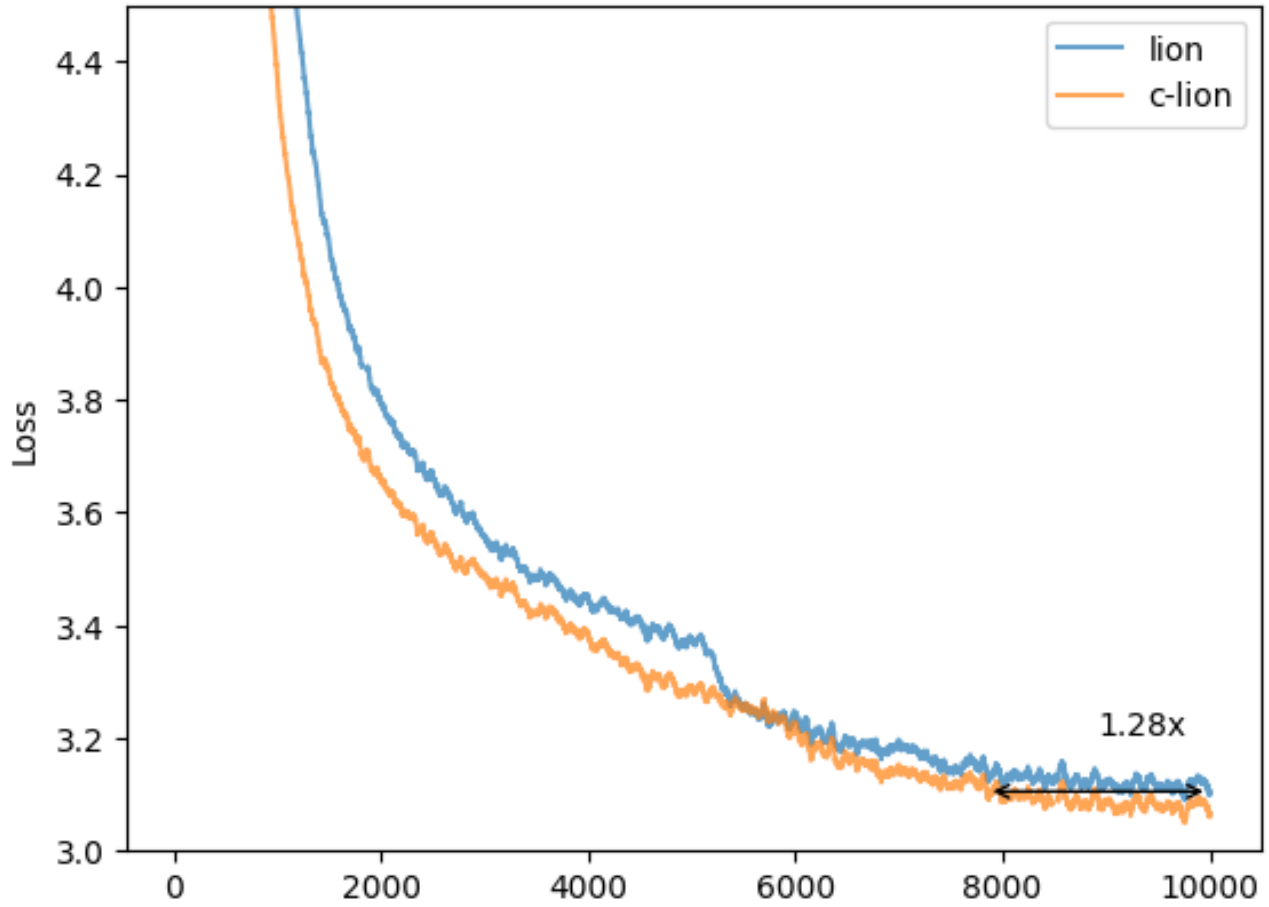


Figure 6: 1.28x speed up on Lion

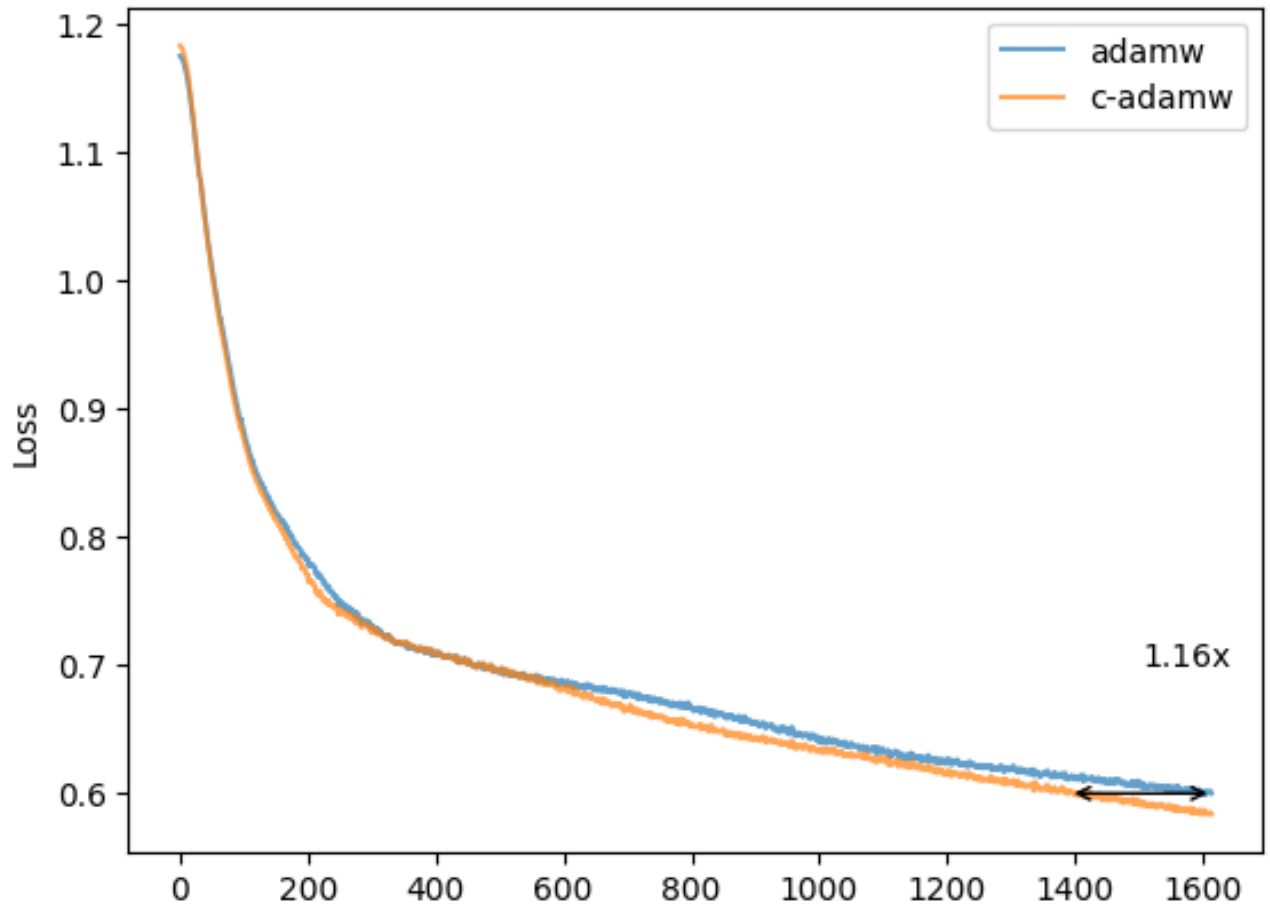


Figure 7: 1.16x speed up on MAE pretraining